Highlights

Safe Multi-Agent Reinforcement Learning for Multi-Robot Control

Shangding Gu[a*], Jakub Grudzien Kuba[b*], Yuanpei Chen[c], Yali Du[d], Long Yang[e], Alois Knoll[a], Yaodong Yang[e]

- The Safe MARL problem is rigorously formulated and analysed—a safe and monotonically improving policy iteration algorithm is derived.
- Deep MARL methods, MACPO and MAPPO-Lagrangian, are proposed.
- Three safe MARL bechmarks are developed: Safe Multi-Agent MuJoCo (Safe MAMuJoCo), Safe Multi-Agent Robosuite (Safe MARobosuite) and Safe Multi-Agent Isaac Gym (Safe MAIG).
- Experiments on the new environment confirm the effectiveness of MACPO and MAPPO-Lagrangian.

Safe Multi-Agent Reinforcement Learning for Multi-Robot Control

Shangding Gu[a*], Jakub Grudzien Kuba[b*], Yuanpei Chen[c], Yali Du[d], Long Yang[e], Alois Knoll[a], Yaodong Yang[e**]

[a]*Department of Computer Science, Technical University of Munich, Germany*
[b]*Department of Statistics, University of Oxford, UK*
[c]*College of Automation Science and Engineering, South China University of Technology, China*
[d]*Department of Informatics, King's College London, UK*
[e]*Institute for AI, Peking University & BIGAI, China*

Abstract

Research on robot control has a long tradition. A challenging problem arising in this domain is how to control multiple robots safely in real-world applications. To our knowledge, no study has considered multi-robot control from the perspective of safe Multi-Agent reinforcement learning (MARL). To fill this gap, in this study, we investigate safe MARL for multi-robot control on cooperative tasks, in which each individual robot has to not only meet its own safety constraints while maximising their reward, but also consider those of others to guarantee safe team behaviours. Firstly, we formulate the safe MARL problem as a constrained Markov game and employ policy Optimisation to solve it theoretically. The proposed algorithm guarantees monotonic improvement in reward and satisfaction of safety constraints at every iteration. Secondly, as approximations to the theoretical solution, we propose two safe multi-agent policy gradient methods: *Multi-Agent Constrained Policy Optimisation* (MACPO) and *MAPPO-Lagrangian*. Thirdly, we develop the first three safe MARL benchmarks—Safe Multi-Agent MuJoCo (Safe MA-MuJoCo), Safe Multi-Agent Robosuite (Safe MARobosuite) and Safe Multi-Agent Isaac Gym (Safe MAIG) to expand the toolkit of MARL and robot control research communities. Finally, experimental results on the three safe

*These authors contributed equally to this work.
**Corresponding author(yaodong.yang@pku.edu.cn).

MARL benchmarks indicate that our methods can achieve state-of-the-art performance in the balance between improving reward and satisfying safety constraints compared with strong baselines. Demos and code are available at the link [1].

Keywords: Constrained Markov Game; Constrained Policy Optimisation; Safe Multi-Agent Benchmarks; Safe Multi-Robot Control

1. Introduction

In the past several decades, traditional control methods have played an important role in multi-robot control, e.g. slide mode control [23], proportional–integral–derivative controller [6] and model predictive control [27] have been widely adopted in the field. However, these methods cannot perform well in environments with unknown dynamics. In fact, the latency of the dynamics may demarcate the limitation of traditional control methods [9]. On the contrary, in recent years, reinforcement learning (RL) has been successfully applied in many tasks, such as transportation schedule [10], traffic signal control [14], the game of Go [41], autonomous driving [28, 19], finance [1], recommender systems [46] and robotics [9]. The robustness of RL to variety of tasks comes from its experience-driven learning that, while relying on a learner's ability to interact with an environment, does not have to possess all of the environment's underlying information. As such, an RL agent formulates a problem of solving a task via maximisation of the reward signal by taking adequate actions [42]. In combination with expressive deep neural networks that model an agent's policy, these methods have made remarkable advancements in the past decade [38, 39, 24].

However, in the context of practical applications, most RL algorithms share a major limitation–they optimise the agents' policies purely for the sake of reward maximisation, completely ignoring safety considerations. For example, in robot control scenarios, it is essential that a robot does not visit certain states, or must not take certain actions, which can be thought of as *unsafe* either for itself or for elements of its background [30, 2]. While the potential danger, *e.g.*, collisions, widely exist in the multi-robot tasks, the difficulty of ascertaining safety is exacerbated in applying multi-agent RL

[1] https://sites.google.com/view/aij-safe-marl/

(MARL). A part of the challenge comes from solving MARL problems themselves [17]. More importantly, however, each individual robot is challenged not only to consider its own safety constraints, which already may conflict its reward maximisation, but also consider the safety constraints of others so that their joint behaviour is guaranteed to be safe. Currently, there are very few solutions that offer effective learning algorithms for safe multi-robot control problems. In this study, we address the problem with theoretical analysis, practical algorithms and three benchmarks.

This study is an extension of our earlier work [20]. Building upon it, firstly, we investigate the safe multi-robot control problem from the safe MARL perspective and develop both theoretical and practical algorithms that solve it. Secondly, we develop sophisticated environments for benchmarking safe MARL algorithms: Safe MAMuJoCo, Safe MARobosuite and Safe MAIG. Finally, we provide experiments to evaluate the effectiveness of our proposed methods, Besides, we also perform parameter studies to show sensitivity of the proposed algorithms to safety-related hyper-parameter changes. To our best knowledge, MACPO and MAPPO-Lagrangian are the first safety-aware model-free MARL algorithms and that work effectively in the challenging tasks with safety constraints.

2. Related Work

Safety is a long-standing pursuit in the development of robotic systems [15]. In safe reinforcement learning, [18], *Constrained Markov Decision Processes* (CMDPs) [4] is commonly employed to describe the safety control problem. At each step of decision making, the environment emits both rewards and costs of the decision, and agents need to maximise reward while avoid violating constraints on costs. Below, we review recent advances on safe RL for both single agent and multi-agent domains.

To tackle the learning problem in CMDPs, [2] introduced *Constrained Policy Optimisation* (CPO) which, like TRPO [38], updates agent's policy under the trust region constraint to maximise surrogate return, meanwhile obeying surrogate cost constraints. However, even more than in the case of TRPO, implementation of a constrained optimisation performed at every iteration of CPO is overwhelmingly cumbersome. An alternative solution is to apply primal-dual methods, giving rise to methods like TRPO-Lagrangian and PPO-Lagrangian [36]. Although these methods achieve impressive performance in terms of safety, their performance in terms of reward is poor

[36]. Another class of algorithms that solves CMDPs is by [12, 13]; these algorithms leverage the theoretical property of the Lyapunov functions and propose safe value iteration and policy gradient procedures. In contrast to CPO, [12, 13] can work with off-policy methods; they also can be trained end-to-end with no need for line search that appears in CPO.

Safe multi-agent learning is an emerging research domain. Despite its importance [40], there are few sound solutions that work with MARL in a model-free setting. For example, CMIX [25] extends QMIX [35] by amending the reward function to take peak constraint violations into account, yet this approach does not come with safety guarantees during training. Furthermore, the majority of methods are designed specifically for learning robotics tasks. For example, the technique of barrier certificates [7, 5, 34] or model predictive shielding [45] from control theory are used to model safety. These methods, however, are derived from the traditional robotics point of view; unlike model-free MARL, they either are supervised learning based approaches, or require specific assumptions on the state space and environment dynamics. Moreover, due to the lack of a benchmark suite for safe MARL algorithms, the generalisation ability of those methods is unclear.

The most related work to ours is Safe Dec-PG [26], in which a primal-dual framework is adopted to find the saddle point between maximising reward and minimising cost. In particular, they proposed a decentralised policy gradient descent-ascent method through a consensus network. However, reaching a consensus equivalently imposes an extra constraint of parameter sharing among neighbouring agents, which could yield suboptimal solutions [21]. Furthermore, multi-agent policy gradient methods can suffer from high variance [22]. In contrast, our methods employ trust region optimisation and do not assume any parameter sharing.

HATRPO, introduced in [21], is the first multi-agent trust region method that enjoys theoretically-justified monotonic improvement guarantee. Its key idea is to make agents follow a sequential policy update scheme so that the expected joint advantage will always be positive, thus increasing reward. In this work, we show how to further develop this theory and derive a protocol which, in addition to the monotonic improvement, also guarantees to satisfy the safety constraints at every iteration during learning. The resulting algorithm (Algorithm 1) successfully attains theoretical guarantees of both monotonic improvement in reward and satisfaction of safety constraints.

3. Problem Formulation: Constrained Markov Game

We formulate the safe MARL problem as a *constrained Markov game* $\langle \mathcal{N}, \mathcal{S}, \mathcal{A}, \mathrm{p}, \rho^0, \gamma, R, \boldsymbol{C}, \boldsymbol{c} \rangle$. Here, $\mathcal{N} = \{1, \ldots, n\}$ is the set of agents, $\mathcal{S}$ is the state space, $\mathcal{A} = \prod_{i=1}^{n} \mathcal{A}^i$ is the product of the agents' action spaces, known as the joint action space, $\mathrm{p} : \mathcal{S} \times \mathcal{A} \times \mathcal{S} \to \mathbb{R}$ is the probabilistic transition function, ρ^0 is the initial state distribution, $\gamma \in [0, 1)$ is the discount factor, $R : \mathcal{S} \times \mathcal{A} \to \mathbb{R}$ is the joint reward function, $\boldsymbol{C} = \{C_j^i\}_{1 \le j \le m^i}^{i \in \mathcal{N}}$ is the set of sets of cost functions (every agent i has m^i cost functions) of the form $C_j^i : \mathcal{S} \times \mathcal{A}^i \to \mathbb{R}$, and finally the set of corresponding cost-constraining values is given by $\boldsymbol{c} = \{c_j^i\}_{1 \le j \le m^i}^{i \in \mathcal{N}}$. At time step t, the agents are in a state s_t, and every agent i takes an action a_t^i according to its policy $\pi^i(\mathrm{a}^i|\mathrm{s}_t)$. Together with other agents' actions, it gives a joint action $\mathbf{a}_t = (\mathrm{a}_t^1, \ldots, \mathrm{a}_t^n)$ and the joint policy $\boldsymbol{\pi}(\mathbf{a}|\mathrm{s}) = \prod_{i=1}^{n} \pi^i(\mathrm{a}^i|\mathrm{s})$. The agents receive the reward $R(\mathrm{s}_t, \mathbf{a}_t)$, meanwhile each agent i pays the costs $C_j^i(\mathrm{s}_t, \mathrm{a}_t^i), \forall j = 1, \ldots, m^i$. The environment then transits to a new state $\mathrm{s}_{t+1} \sim \mathrm{p}(\cdot|\mathrm{s}_t, \mathbf{a}_t)$. In this paper, we consider a *fully-cooperative* setting where all agents share the same reward function, aiming to maximise the expected total reward of

$$J(\boldsymbol{\pi}) \triangleq \mathbb{E}_{\mathrm{s}_0 \sim \rho^0, \mathbf{a}_{0:\infty} \sim \boldsymbol{\pi}, \mathrm{s}_{1:\infty} \sim \mathrm{p}} \Big[\sum_{t=0}^{\infty} \gamma^t R(\mathrm{s}_t, \mathbf{a}_t) \Big],$$

meanwhile trying to satisfy every agent i's safety constraints, written as

$$J_j^i(\boldsymbol{\pi}) \triangleq \mathbb{E}_{\mathrm{s}_0 \sim \rho^0, \mathbf{a}_{0:\infty} \sim \boldsymbol{\pi}, \mathrm{s}_{1:\infty} \sim \mathrm{p}} \Big[\sum_{t=0}^{\infty} \gamma^t C_j^i(\mathrm{s}_t, \mathrm{a}_t^i) \Big] \le c_j^i, \qquad \forall j = 1, \ldots, m^i. \quad (1)$$

We define the state-action value and the state-value functions in terms of reward as

$$Q_{\boldsymbol{\pi}}(s, \boldsymbol{a}) \triangleq \mathbb{E}_{\mathrm{s}_{1:\infty} \sim \mathrm{p}, \mathbf{a}_{1:\infty} \sim \boldsymbol{\pi}} \Big[\sum_{t=0}^{\infty} \gamma^t R(\mathrm{s}_t, \mathbf{a}_t) \big| \mathrm{s}_0 = s, \mathbf{a}_0 = \boldsymbol{a} \Big],$$
$$V_{\boldsymbol{\pi}}(s) \triangleq \mathbb{E}_{\mathbf{a} \sim \boldsymbol{\pi}} \big[Q_{\boldsymbol{\pi}}(s, \mathbf{a}) \big].$$

The joint policies $\boldsymbol{\pi}$ that satisfy the Inequality (1) are referred to as **feasible**. Notably, in the above formulation, although the action a_t^i of agent i does not directly influence the costs $\{C_j^k(\mathrm{s}_t, \mathrm{a}_t^k)\}_{j=1}^{m^k}$ of other agents $k \neq i$, the action a_t^i will implicitly influence their total costs due to the dependence on the next

state s_{t+1}. We believe that this formulation realistically describes multi-agent interactions in the real-world; an action of an agent has an instantaneous effect on the system only locally, but the rest of agents may suffer from its consequences at later stages. For example, we consider a car that crosses on the red light: although other cars may not be at risk of riding into pedestrians immediately, the induced traffic may cause hazards soon later. For the j^{th} cost function of agent i, we define the j^{th} state-action cost value function and the state cost value function as

$$Q^i_{j,\boldsymbol{\pi}}(s, a^i) \triangleq \mathbb{E}_{\mathbf{a}^{-i}\sim\boldsymbol{\pi}^{-i},\mathrm{s}_{1:\infty}\sim\mathrm{p},\mathbf{a}_{1:\infty}\sim\boldsymbol{\pi}}\Big[\sum_{t=0}^{\infty}\gamma^t C^i_j(\mathrm{s}_t,\mathrm{a}^i_t)\;\Big|\;\mathrm{s}_0=s,\mathrm{a}^i_0=a^i\Big],$$

$$V^i_{j,\boldsymbol{\pi}}(s) \triangleq \mathbb{E}_{\mathbf{a}\sim\boldsymbol{\pi},\mathrm{s}_{1:\infty}\sim\mathrm{p},\mathbf{a}_{1:\infty}\sim\boldsymbol{\pi}}\Big[\sum_{t=0}^{\infty}\gamma^t C^i_j(\mathrm{s}_t,\mathrm{a}^i_t)\;\Big|\;\mathrm{s}_0=s\Big].$$

Notably, the cost value functions $Q^i_{j,\boldsymbol{\pi}}$ and $V^i_{j,\boldsymbol{\pi}}$, although similar to traditional $Q_{\boldsymbol{\pi}}$ and $V_{\boldsymbol{\pi}}$, involve extra indices i and j; the superscript i denotes an agent, and the subscript j denotes its j^{th} cost.

Throughout this work, we pay a close attention to the contribution to performance from different subsets of agents, therefore, we introduce the following notations. We denote an arbitrary subset $\{i_1,\ldots,i_h\}$ of agents as $i_{1:h}$; we write $-i_{1:h}$ to refer to its complement. Given the agent subset $i_{1:h}$, we define the *multi-agent state-action value function*:

$$Q^{i_{1:h}}_{\boldsymbol{\pi}}(s,\boldsymbol{a}^{i_{1:h}}) \triangleq \mathbb{E}_{\mathbf{a}^{-i_{1:h}}\sim\boldsymbol{\pi}^{-i_{1:h}}}\left[Q_{\boldsymbol{\pi}}(\mathrm{s},\boldsymbol{a}^{i_{1:h}},\mathbf{a}^{-i_{1:h}})\right].$$

On top of it, the *multi-agent advantage function* [2] is defined as follows,

$$A^{i_{1:h}}_{\boldsymbol{\pi}}\big(s,\boldsymbol{a}^{j_{1:k}},\boldsymbol{a}^{i_{1:h}}\big) \triangleq Q^{j_{1:k},i_{1:h}}_{\boldsymbol{\pi}}\big(s,\boldsymbol{a}^{j_{1:k}},\boldsymbol{a}^{i_{1:h}}\big) - Q^{j_{1:k}}_{\boldsymbol{\pi}}\big(s,\boldsymbol{a}^{j_{1:k}}\big). \tag{2}$$

An interesting fact about the above multi-agent advantage function is that any advantage $A^{i_{1:h}}_{\boldsymbol{\pi}}$ can be written as a sum of sequentially-unfolding multi-agent advantages of individual agents, that is,

[2] We would like to highlight that these multi-agent functions of $Q^{i_{1:h}}_{\boldsymbol{\pi}}$ and $A^{i_{1:h}}_{\boldsymbol{\pi}}$, although involve agents in superscripts, describe values *w.r.t* the reward rather than costs since they do not involve cost subscripts.

Lemma 1 (Multi-Agent Advantage Decomposition, [22]). *For any state $s \in \mathcal{S}$, subset of agents $i_{1:h} \subseteq \mathcal{N}$, and joint action $\boldsymbol{a}^{i_{1:h}}$, the following identity holds*

$$A_{\boldsymbol{\pi}}^{i_{1:h}}\left(s, \boldsymbol{a}^{i_{1:h}}\right) = \sum_{j=1}^{h} A_{\boldsymbol{\pi}}^{i_j}\left(s, \boldsymbol{a}^{i_{1:j-1}}, a^{i_j}\right).$$

Proof. We write the multi-agent advantage as in its definition, and expand it in a telescoping sum.

$$\begin{aligned} A_{\boldsymbol{\pi}}^{i_{1:h}}\left(s, \boldsymbol{a}^{i_{1:h}}\right) &= Q_{\boldsymbol{\pi}}^{i_{1:h}}\left(s, \boldsymbol{a}^{i_{1:h}}\right) - V_{\boldsymbol{\pi}}\left(s\right) \\ &= \sum_{j=1}^{h}\left[Q_{\boldsymbol{\pi}}^{i_{1:j}}\left(s, \boldsymbol{a}^{i_{1:j}}\right) - Q_{\boldsymbol{\pi}}^{i_{1:j-1}}\left(s, \boldsymbol{a}^{i_{1:j-1}}\right)\right] \\ &= \sum_{j=1}^{h} A_{\boldsymbol{\pi}}^{i_j}\left(s, \boldsymbol{a}^{i_{1:j-1}}, a^{i_j}\right). \end{aligned}$$

□

4. Multi-Agent Constrained Policy Optimisation

In this section, we first present a theoretically-justified safe multi-agent policy iteration procedure that leverages multi-agent trust region learning and constrained policy optimisation to solve constrained Markov games. Based on this, we propose two practical deep MARL algorithms, enabling optimising neural-network based policies that satisfy safety constraints. Throughout this work, we refer the symbols $\boldsymbol{\pi}$ and $\bar{\boldsymbol{\pi}}$ to be the "current" and the "new" joint policies, respectively.

4.1. Multi-Agent Trust Region Learning With Constraints

[21] introduced the first multi-agent trust region method—HATRPO—that enjoys theoretically-justified monotonic improvement guarantee. Specifically, it relies on the multi-agent advantage decomposition in Lemma 1, and the "surrogate" return that is given as follows.

Definition 1. *Let $\boldsymbol{\pi}$ be a joint policy, $\bar{\boldsymbol{\pi}}^{i_{1:h-1}}$ be some other joint policy of agents $i_{1:h-1}$, and $\hat{\pi}^{i_h}$ be a policy of agent i_h. Then we define*

$$L_{\boldsymbol{\pi}}^{i_{1:h}}\left(\bar{\boldsymbol{\pi}}^{i_{1:h-1}}, \hat{\pi}^{i_h}\right) \triangleq \mathbb{E}_{\mathrm{s}\sim\rho_{\boldsymbol{\pi}}, \mathbf{a}^{i_{1:h-1}}\sim\bar{\boldsymbol{\pi}}^{i_{1:h-1}}, \mathrm{a}^{i_h}\sim\hat{\pi}^{i_h}}\left[A_{\boldsymbol{\pi}}^{i_h}\left(\mathrm{s}, \mathbf{a}^{i_{1:h-1}}, \mathrm{a}^{i_h}\right)\right].$$

With the above definition, we see that Lemma 1 allows for decomposing the joint surrogate return $L_{\boldsymbol{\pi}}(\bar{\boldsymbol{\pi}}) \triangleq \mathbb{E}_{\mathrm{s}\sim\rho_{\boldsymbol{\pi}},\mathbf{a}\sim\bar{\boldsymbol{\pi}}}[A_{\boldsymbol{\pi}}(\mathrm{s},\mathbf{a})]$ into a sum over surrogates of $L_{\boldsymbol{\pi}}^{i_{1:h}}(\bar{\boldsymbol{\pi}}^{i_{1:h-1}}, \bar{\pi}^{i_h})$, for $h = 1,\dots,n$. This can be used to justify that if agents, with a joint policy $\boldsymbol{\pi}$, update their policies by following a *sequential update scheme*, that is, if each agent in the subset $i_{1:h}$ sequentially solves the following optimisation problem:

$$\begin{aligned} \bar{\pi}^{i_h} &= \arg\max_{\hat{\pi}^{i_h}} L_{\boldsymbol{\pi}}^{i_{1:h}}\left(\bar{\boldsymbol{\pi}}^{i_{1:h-1}}, \hat{\pi}^{i_h}\right) - \nu D_{\mathrm{KL}}^{\max}\left(\pi^{i_h}, \hat{\pi}^{i_h}\right), \\ &\text{where} \quad \nu = \frac{4\gamma \max_{s,\boldsymbol{a}} |A_{\boldsymbol{\pi}}(s,\boldsymbol{a})|}{(1-\gamma)^2}, \\ \text{and} \quad & D_{\mathrm{KL}}^{\max}(\pi^{i_h}, \hat{\pi}^{i_h}) \triangleq \max_s D_{\mathrm{KL}}(\pi^{i_h}(\cdot|s), \hat{\pi}^{i_h}(\cdot|s)), \end{aligned} \tag{3}$$

then the resulting joint policy $\bar{\boldsymbol{\pi}}$ will surely improve the expected return, i.e., $J(\bar{\boldsymbol{\pi}}) \geq J(\boldsymbol{\pi})$ (see the proof in [21, Lemma 2]). We know that due to the penalty term $D_{\mathrm{KL}}^{\max}(\pi^{i_h}, \hat{\pi}^{i_h})$, the new policy $\bar{\pi}^{i_h}$ will stay close (*w.r.t* max-KL distance) to π^{i_h}.

For the safety constraints, we can extend Definition 1 to incorporate the "surrogate" cost, thus allowing us to study the cost functions in addition to the return.

Definition 2. *Let $\boldsymbol{\pi}$ be a joint policy, and $\bar{\pi}^i$ be some other policy of agent i. Then, for any of its costs of index $j \in \{1,\dots,m^i\}$, we define*

$$L_{j,\boldsymbol{\pi}}^i\left(\bar{\pi}^i\right) = \mathbb{E}_{\mathrm{s}\sim\rho_{\boldsymbol{\pi}},\mathrm{a}^i\sim\bar{\pi}^i}\left[A_{j,\boldsymbol{\pi}}^i\left(\mathrm{s},\mathrm{a}^i\right)\right].$$

By generalising the result about the surrogate return in Equation (1), we can derive how the expected costs change when the agents update their policies. Specifically, we provide the following lemma.

Lemma 2. *Let $\boldsymbol{\pi}$ and $\bar{\boldsymbol{\pi}}$ be joint policies. Let $i \in \mathcal{N}$ be an agent, and $j \in \{1,\dots,m^i\}$ be an index of one of its costs. The following inequality holds*

$$J_j^i(\bar{\boldsymbol{\pi}}) \leq J_j^i(\boldsymbol{\pi}) + L_{j,\boldsymbol{\pi}}^i\left(\bar{\pi}^i\right) + \nu_j^i \sum_{h=1}^{n} D_{KL}^{max}\left(\pi^h, \bar{\pi}^h\right),$$

where $\nu_j^i = \frac{4\gamma \max_{s,a^i} |A_{j,\boldsymbol{\pi}}^i(s,a^i)|}{(1-\gamma)^2}$.

Proof. From the upper-bound version of Theorem 1 of [38] applied to joint policies $\boldsymbol{\pi}$ and $\bar{\boldsymbol{\pi}}$, we conclude that

$$J_j^i(\bar{\boldsymbol{\pi}}) \leq J_j^i(\boldsymbol{\pi}) + \mathbb{E}_{\mathrm{s}\sim\rho_{\boldsymbol{\pi}},\mathbf{a}\sim\bar{\boldsymbol{\pi}}}\left[A_{j,\boldsymbol{\pi}}^i(\mathrm{s},\mathrm{a}^i)\right] + \frac{4\alpha^2\gamma\max_{s,a^i}|A_{j,\boldsymbol{\pi}}^i(s,a^i)|}{(1-\gamma)^2},$$

where $\alpha = D_{\mathrm{TV}}^{\max}(\boldsymbol{\pi},\bar{\boldsymbol{\pi}}) = \max_s D_{\mathrm{TV}}(\boldsymbol{\pi}(\cdot|s),\bar{\boldsymbol{\pi}}(\cdot|s))$.

Using the inequality $D_{\mathrm{TV}}(p,q)^2 \leq D_{\mathrm{KL}}(p,q)$ [33, 38], we obtain

$$J_j^i(\bar{\boldsymbol{\pi}}) \leq J_j^i(\boldsymbol{\pi}) + \mathbb{E}_{\mathrm{s}\sim\rho_{\boldsymbol{\pi}},\mathbf{a}\sim\bar{\boldsymbol{\pi}}}\left[A_{j,\boldsymbol{\pi}}^i(\mathrm{s},\mathrm{a}^i)\right] + \frac{4\gamma\max_{s,a^i}|A_{j,\boldsymbol{\pi}}^i(s,a^i)|}{(1-\gamma)^2}D_{\mathrm{KL}}^{\max}(\boldsymbol{\pi},\bar{\boldsymbol{\pi}}),$$

where $D_{\mathrm{KL}}^{\max}(\boldsymbol{\pi},\bar{\boldsymbol{\pi}}) = \max_s D_{\mathrm{KL}}(\boldsymbol{\pi}(\cdot|s),\bar{\boldsymbol{\pi}}(\cdot|s))$.

Notice now that we have $\mathbb{E}_{\mathrm{s}\sim\rho_{\boldsymbol{\pi}},\mathbf{a}\sim\bar{\boldsymbol{\pi}}}\left[A_{j,\boldsymbol{\pi}}^i(\mathrm{s},\mathrm{a}^i)\right] = \mathbb{E}_{\mathrm{s}\sim\rho_{\boldsymbol{\pi}},\mathrm{a}^i\sim\bar{\pi}^i}\left[A_{j,\boldsymbol{\pi}}^i(\mathrm{s},\mathrm{a}^i)\right]$ as the action of agents other that i do not change the value of the variable inside of the expectation. Furthermore

$$\begin{aligned} D_{\mathrm{KL}}^{\max}(\boldsymbol{\pi},\bar{\boldsymbol{\pi}}) &= \max_s D_{\mathrm{KL}}(\boldsymbol{\pi}(\cdot|s),\bar{\boldsymbol{\pi}}(\cdot|s)) = \max_s\left(\sum_{l=1}^n D_{\mathrm{KL}}\left(\pi^l(\cdot|s),\bar{\pi}^l(\cdot|s)\right)\right) \\ &\leq \sum_{l=1}^n \max_s D_{\mathrm{KL}}\left(\pi^l(\cdot|s),\bar{\pi}^l(\cdot|s)\right) = \sum_{l=1}^n D_{\mathrm{KL}}^{\max}\left(\pi^l,\bar{\pi}^l\right). \end{aligned} \tag{4}$$

Setting $\nu_j^i = \frac{4\gamma\max_{s,a^i}|A_{j,\boldsymbol{\pi}}^i(s,a^i)|}{(1-\gamma)^2}$, we finally obtain

$$J_j^i(\bar{\boldsymbol{\pi}}) \leq J_j^i(\boldsymbol{\pi}) + L_{j,\boldsymbol{\pi}}^i\left(\bar{\pi}^i\right) + \nu_j^i\sum_{l=1}^n D_{\mathrm{KL}}^{\max}\left(\pi^l,\bar{\pi}^l\right).$$

□

The above lemma suggests that, as long as the distances between the policies π^h and $\bar{\pi}^h$, $\forall h \in \mathcal{N}$, are sufficiently small, then the change in the j^{th} cost of agent i, i.e., $J_j^i(\bar{\boldsymbol{\pi}}) - J_j^i(\boldsymbol{\pi})$, is controlled by the surrogate $L_{j,\boldsymbol{\pi}}^i(\bar{\pi}^i)$. Importantly, this surrogate is independent of other agents' new policies. Hence, when the changes in policies of all agents are sufficiently small, each agent i can learn a better policy $\bar{\pi}^i$ by only considering its own surrogate return and surrogate costs. To summarise, we provide Algorithm 1 that guarantees both safety constraints satisfaction and monotonic performance improvement.

Algorithm 1: Safe Multi-Agent Policy Iteration with Monotonic Improvement Property

Initialise a safe joint policy $\boldsymbol{\pi}_0 = (\pi_0^1, \dots, \pi_0^n)$.
for $k = 0, 1, \dots$ **do**
  Compute the advantage functions $A_{\boldsymbol{\pi}_k}(s, \boldsymbol{a})$ and $A^i_{j,\boldsymbol{\pi}_k}(s, a^i)$, for all state-(joint)action pairs $(s, \boldsymbol{a})$, agents i, and constraints $j \in \{1, \dots, m^i\}$.
  Compute $\nu = \frac{4\gamma \max_{s,\boldsymbol{a}} |A_{\boldsymbol{\pi}_k}(s,\boldsymbol{a})|}{(1-\gamma)^2}$, and $\nu^i_j = \frac{4\gamma \max_{s,a^i} |A^i_{j,\boldsymbol{\pi}_k}(s,a^i)|}{(1-\gamma)^2}$, $\forall i \in \mathcal{N}, j = 1, \dots, m^i$.
  Draw a permutaion $i_{1:n}$ of agents at random.
  for $h = 1 : n$ **do**
    Compute the radius of the KL-constraint δ^{i_h} // *see Equation (6) for the setup of* δ^{i_h}.
    Make an update $\pi^{i_h}_{k+1} = \arg\max_{\pi^{i_h} \in \overline{\Pi}^{i_h}} \left[L^{i_{1:h}}_{\boldsymbol{\pi}_k}\left(\pi^{i_{1:h-1}}_{k+1}, \pi^{i_h}\right) - \nu D^{\max}_{\mathrm{KL}}\left(\pi^{i_h}_k, \pi^{i_h}\right)\right]$, where $\overline{\Pi}^{i_h}$ is a subset of safe policies of agent i_h, given by

$$\begin{aligned}\overline{\Pi}^{i_h} = \Big\{ \pi^{i_h} \in \Pi^{i_h} \;\Big|\; & D^{\max}_{\mathrm{KL}}(\pi^{i_h}_k, \pi^{i_h}) \le \delta^{i_h}, \text{ and} \\ & J^{i_h}_j(\boldsymbol{\pi}_k) + L^{i_h}_{j,\boldsymbol{\pi}_k}(\pi^{i_h}) + \nu^{i_h}_j D^{\max}_{\mathrm{KL}}(\pi^{i_h}_k, \pi^{i_h}) \le \\ & c^{i_h}_j - \sum_{l=1}^{h-1} \nu^{i_l}_j D^{\max}_{\mathrm{KL}}(\pi^{i_l}_k, \pi^{i_l}), \forall j = 1, \dots, m^{i_h} \Big\}. \end{aligned} \tag{5}$$

  end for
end for

In this algorithm, in addition to sequentially maximising agents' surrogate returns, the agents must assure that their surrogate costs stay below the corresponding safety thresholds. Meanwhile, they have to constrain their policy search to small local neighbourhoods (*w.r.t* max-KL distance). As such, Algorithm 1 demonstrates two desirable properties: reward performance improvement and satisfaction of safety constraints, as stated by Theorem 1.

In Algorithm 1, we compute the size of KL constraint as

$$\delta^{i_h} = \min \left\{ \min_{l \leq h-1} \min_{1 \leq j \leq m^l} \frac{c_j^{i_l} - J_j^{i_l}(\boldsymbol{\pi}_k) - L_{j,\boldsymbol{\pi}_k}^{i_l}(\pi_{k+1}^{i_l}) - \nu_j^{i_l} \sum_{u=1}^{h-1} D_{\mathrm{KL}}^{\max}(\pi_k^u, \pi_{k+1}^u)}{\nu_j^{i_l}}, \right. \\ \left. \min_{l \geq h+1} \min_{1 \leq j \leq m^l} \frac{c_j^{i_l} - J_j^{i_l}(\boldsymbol{\pi}_k) - \nu_j^{i_l} \sum_{u=1}^{h-1} D_{\mathrm{KL}}^{\max}(\pi_k^u, \pi_{k+1}^u)}{\nu_j^{i_l}} \right\}. \tag{6}$$

Note that δ^{i_1} (i.e., $h = 1$) is guaranteed to be non-negative if $\boldsymbol{\pi}_k$ satisfies safety constraints; that is because then $c_j^{i_l} \geq J_j^{i_l}(\boldsymbol{\pi}_k)$ for all l and j, and the set $\{l \mid l{<}h\}$ is empty.

This formula for δ^{i_h}, combined with Lemma 2, assures that the policies π^{i_h} within δ^{i_h} max-KL distance from $\pi_k^{i_h}$ will not violate other agents' safety constraints, as long as the base joint policy $\boldsymbol{\pi}_k$ did not violate them (which assures $\delta^{i_1} \geq 0$). To see this, notice that for every $l = 1, \ldots, h-1$, and $j = 1, \ldots, m^l$,

$$D_{\mathrm{KL}}^{\max}(\pi_k^{i_h}, \pi^{i_h}) \leq \delta^{i_h} \leq \frac{c_j^{i_l} - J_j^{i_l}(\boldsymbol{\pi}_k) - L_{j,\boldsymbol{\pi}_k}^{i_l}(\pi_{k+1}^{i_l}) - \nu_j^{i_l} \sum_{u=1}^{h-1} D_{\mathrm{KL}}^{\max}(\pi_k^u, \pi_{k+1}^u)}{\nu_j^{i_l}},$$

$$\text{implies} \quad J_j^{i_l}(\boldsymbol{\pi}_k) + L_{j,\boldsymbol{\pi}_k}^{i_l}(\pi_{k+1}^{i_l}) + \nu_j^{i_l} \sum_{u=1}^{h-1} D_{\mathrm{KL}}^{\max}(\pi_k^u, \pi_{k+1}^u) + \nu_j^{i_l} D_{\mathrm{KL}}^{\max}(\pi_k^{i_h}, \pi^{i_h}) \leq c_j^{i_l}.$$

By Lemma 2, the left-hand side of the above inequality is an upper bound of $J_j^{i_l}(\pi_{k+1}^{i_{1:h-1}}, \pi^{i_h}, \pi_k^{-i_{1:h}})$, which implies that the update of agent i_h does not violate the constraint of $J_j^{i_l}$. The fact that the constraints of $J_j^{i_l}$ for $l \geq h+1$ are not violated, i.e.,

$$J_j^{i_l}(\boldsymbol{\pi}_k) + \nu_j^{i_l} \sum_{u=1}^{h-1} D_{\mathrm{KL}}^{\max}(\pi_k^u, \pi_{k+1}^u) + \nu_j^{i_l} D_{\mathrm{KL}}^{\max}(\pi_k^{i_h}, \pi^{i_h}) \leq c_j^{i_l}, \tag{7}$$

is analogous.

Theorem 1. *If a sequence of joint policies $(\boldsymbol{\pi}_k)_{k=0}^{\infty}$ is obtained from Algorithm 1, then it has the monotonic improvement property, $J(\boldsymbol{\pi}_{k+1}) \geq J(\boldsymbol{\pi}_k)$, as well as it satisfies the safety constraints, $J_j^i(\boldsymbol{\pi}_k) \leq c_j^i$, for all $k \in \mathbb{N}, i \in \mathcal{N}$, and $j \in \{1, \ldots, m^i\}$.*

Proof. Safety constraints are assured to be met if the agents' update size is bounded by Equation (6). It suffices to show the monotonic improvement property. By Theorem 1 from [38], we have

$$J(\boldsymbol{\pi}_{k+1}) \geq J(\boldsymbol{\pi}_k) + \mathbb{E}_{\mathrm{s}\sim\rho_{\boldsymbol{\pi}_k}, \mathbf{a}\sim\boldsymbol{\pi}_{k+1}}\left[A_{\boldsymbol{\pi}_k}(\mathrm{s}, \mathbf{a})\right] - \nu D_{\mathrm{KL}}^{\max}(\boldsymbol{\pi}_k, \boldsymbol{\pi}_{k+1}),$$

which by Equation 4 is lower-bounded by

$$\geq J(\boldsymbol{\pi}_k) + \mathbb{E}_{\mathrm{s}\sim\rho_{\boldsymbol{\pi}_k}, \mathbf{a}\sim\boldsymbol{\pi}_{k+1}}\left[A_{\boldsymbol{\pi}_k}(\mathrm{s}, \mathbf{a})\right] - \sum_{h=1}^{n} \nu D_{\mathrm{KL}}^{\max}(\pi_k^{i_h}, \pi_{k+1}^{i_h})$$

which by Lemma 1 equals

$$= J(\boldsymbol{\pi}_k) + \sum_{h=1}^{n} \mathbb{E}_{\mathrm{s}\sim\rho_{\boldsymbol{\pi}_k}, \mathbf{a}^{i_{1:h}}\sim\boldsymbol{\pi}_{k+1}^{i_{1:h}}}\left[A_{\boldsymbol{\pi}_k}^{i_h}(\mathrm{s}, \mathbf{a}^{i_{1:h-1}}, \mathrm{a}^{i_h})\right] - \sum_{h=1}^{n} \nu D_{\mathrm{KL}}^{\max}(\pi_k^{i_h}, \pi_{k+1}^{i_h})$$

$$= J(\boldsymbol{\pi}_k) + \sum_{h=1}^{n} \left(L_{\boldsymbol{\pi}_k}^{i_{1:h}}(\boldsymbol{\pi}_{k+1}^{i_{1:h-1}}, \pi_{k+1}^{i_h}) - \nu D_{\mathrm{KL}}^{\max}(\pi_k^{i_h}, \pi_{k+1}^{i_h})\right), \tag{8}$$

and as for every h, $\pi_{k+1}^{i_h}$ is the argmax, this is lower-bounded by

$$\geq J(\boldsymbol{\pi}_k) + \sum_{h=1}^{n} \left(L_{\boldsymbol{\pi}_k}^{i_{1:h}}(\boldsymbol{\pi}_{k+1}^{i_{1:h-1}}, \pi_k^{i_h}) - \nu D_{\mathrm{KL}}^{\max}(\pi_k^{i_h}, \pi_k^{i_h})\right),$$

which, as follows from Definition 1, equals

$$= \mathcal{J}(\boldsymbol{\pi}_k) + \sum_{h=1}^{n} 0 = J(\boldsymbol{\pi}_k), \text{ which finishes the proof.}$$

□

Theorem 1 assures that agents that follow Algorithm 1 will not only explore safe policies; meanwhile, every new policy will be guaranteed to result in performance improvement. These two properties hold under the condition that only restrictive policy updates are made; this is due to the KL-penalty term in every agent's objective (i.e., $\nu D_{\mathrm{KL}}^{\max}(\pi_k^{i_h}, \pi^{i_h})$), as well as the constraints on cost surrogates (i.e., the conditions in $\overline{\Pi}^{i_h}$). In practice, it can be intractable to evaluate $D_{\mathrm{KL}}\big(\pi_k^{i_h}(\cdot|s), \pi^{i_h}(\cdot|s)\big)$ at every state in order to

compute $D_{\mathrm{KL}}^{\max}(\pi_k^{i_h}, \pi^{i_h})$. In the following subsections, we describe how to approximate Algorithm 1 in the case of parameterised policies.

4.2. MACPO: Multi-Agent Constrained Policy Optimisation

In this section, we focus on the practical implementation where large state and action spaces prevent agents from designating policies $\pi^i(\cdot|s)$ for each state separately. To handle this, we parameterise each agent's policy $\pi^i_{\theta^i}$ by a neural network with parameter θ^i. Correspondingly, the joint policies $\boldsymbol{\pi}_{\boldsymbol{\theta}}$ are parametrised by $\boldsymbol{\theta} = (\theta^1, \ldots, \theta^n)$.

At each iteration of Algorithm 1, every agent i_h maximises its surrogate return with a KL-penalty, subject to surrogate cost constraint. Yet, direct computation of the max-KL constraint is intractable in practical settings, as it would require computation of KL-divergence at every single state. Instead, we relax it by adopting a form of expected KL-constraint

$$\overline{D}_{\mathrm{KL}}(\pi_k^{i_h}, \pi^{i_h}) \leq \delta,$$

where $\overline{D}_{\mathrm{KL}}(\pi_k^{i_h}, \pi^{i_h}) \triangleq \mathbb{E}_{\mathrm{s}\sim\rho_{\boldsymbol{\pi}_k}}\left[D_{\mathrm{KL}}(\pi_k^{i_h}(\cdot|\mathrm{s}), \pi^{i_h}(\cdot|\mathrm{s}))\right]$.

We approximate these expectations by sampling. As a result, the optimisation problem solved by agent i_h can be written as

$$\begin{aligned}
\theta_{k+1}^{i_h} = \arg\max_{\theta^{i_h}} & \mathbb{E}_{\mathrm{s}\sim\rho_{\boldsymbol{\pi}_{\boldsymbol{\theta}_k}}, \mathbf{a}^{i_{1:h-1}}\sim\boldsymbol{\pi}^{i_{1:h-1}}_{\boldsymbol{\theta}^{i_{1:h-1}}_{k+1}}, \mathrm{a}^{i_h}\sim\pi^{i_h}_{\theta^{i_h}}}\left[A^{i_h}_{\boldsymbol{\pi}_{\boldsymbol{\theta}_k}}\left(\mathrm{s}, \mathbf{a}^{i_{1:h-1}}, \mathrm{a}^{i_h}\right)\right] \\
\text{s.t.} \quad & J_j^{i_h}\left(\boldsymbol{\pi}_{\boldsymbol{\theta}_k}\right) + \mathbb{E}_{\mathrm{s}\sim\rho_{\boldsymbol{\pi}_{\boldsymbol{\theta}_k}}, \mathrm{a}^{i_h}\sim\pi^{i_h}_{\theta^{i_h}_k}}\left[A^{i_h}_{j,\boldsymbol{\pi}_{\boldsymbol{\theta}_k}}\left(\mathrm{s}, \mathrm{a}^{i_h}\right)\right] \leq c_j^{i_h}, \ \forall j \in \{1, \ldots, m^{i_h}\}, \\
& \text{and} \ \ \overline{D}_{\mathrm{KL}}\left(\pi_k^{i_h}, \pi^{i_h}\right) \leq \delta. \qquad (9)
\end{aligned}$$

To solve this problem, we approximate Equation (9) with the Taylor expansion of the optimisation objective and cost constraints up to the first order, and the KL-divergence up to the second order. Consequently, the optimisation problem (9) can be written as

$$\begin{aligned}
\theta_{k+1}^{i_h} = \arg\max_{\theta^{i_h}} & \left(\boldsymbol{g}^{i_h}\right)^T\left(\theta^{i_h} - \theta_k^{i_h}\right) \\
\text{s.t.} \quad & d_j^{i_h} + \left(\boldsymbol{b}_j^{i_h}\right)^T\left(\theta^{i_h} - \theta_k^{i_h}\right) \leq 0, \quad j = 1, \ldots, m \\
& \frac{1}{2}\left(\theta^{i_h} - \theta_k^{i_h}\right)^T \boldsymbol{H}^{i_h}\left(\theta^{i_h} - \theta_k^{i_h}\right) \leq \delta, \qquad (10)
\end{aligned}$$

where $\boldsymbol{g}^{i_h}$ is the gradient of the objective of agent i_h in Equation (9),

$$d_j^i = J_j^i(\boldsymbol{\pi}_{\boldsymbol{\theta}_k}) - c_j^i,$$

and $\boldsymbol{H}^{i_h} = \nabla^2_{\theta^{i_h}} \overline{D}_{\mathrm{KL}}(\pi^{i_h}_{\theta^{i_h}_k}, \pi^{i_h})\big|_{\theta^{i_h}=\theta^{i_h}_k}$, is the Hessian of the average KL divergence of agent i_h, and $\boldsymbol{b}_j^{i_h}$ is the gradient of agent of the j^{th} constraint of agent i_h.

Similar to [2] and [11], we can take a primal-dual optimisation approach to solve the linear quadratic optimisation in Equation (10). Specifically, the dual form is given by

$$\max_{\lambda^{i_h}\geq 0, \mathbf{v}^{i_h}\geq 0} \frac{-1}{2\lambda^{i_h}}\left[(\boldsymbol{g}^{i_h})^T(\boldsymbol{H}^{i_h})^{-1}\boldsymbol{g}^{i_h} - 2(\boldsymbol{r}^{i_h})^T\mathbf{v}^{i_h} + (\mathbf{v}^{i_h})^T\boldsymbol{S}^{i_h}\right] + (\mathbf{v}^{i_h})^T\boldsymbol{c}^{i_h} - \frac{\lambda^{i_h}\delta}{2}, \tag{11}$$

where $\boldsymbol{B}^{i_h} = \left[\boldsymbol{b}_1^{i_h}, \ldots, \boldsymbol{b}_m^{i_h}\right]$, $\boldsymbol{r}^{i_h} \triangleq (\boldsymbol{g}^{i_h})^T(\boldsymbol{H}^{i_h})^{-1}\boldsymbol{B}^{i_h}$, $\boldsymbol{S}^{i_h} \triangleq (\boldsymbol{B}^{i_h})^T(\boldsymbol{H}^{i_h})^{-1}\boldsymbol{B}^{i_h}$.

Given the solution to the dual form in Equation (11), i.e., $\lambda_*^{i_h}$ and $\mathbf{v}_*^{i_h}$, the solution to the primal problem in Equation (10) can thus be written by

$$\theta_*^{i_h} = \theta_k^{i_h} + \frac{1}{\lambda_*^{i_h}}\left(\boldsymbol{H}^{i_h}\right)^{-1}\left(\boldsymbol{g}^{i_h} - \boldsymbol{B}^{i_h}\mathbf{v}_*^{i_h}\right).$$

See Appendix Appendix B for derivation. In practice, we use backtracking line search starting at $1/\lambda_*^{i_h}$ to choose the step size of the above update. Furthermore, we note that the optimisation step in Equation (10) is an approximation to the original problem from Equation (9); therefore, it is possible that an infeasible policy $\pi_{\theta^{i_h}_{k+1}}$ will be generated. Fortunately, as the policy optimisation takes place in the trust region of $\pi^{i_h}_{\theta^{i_h}_k}$, the size of update is small, and a feasible policy can be easily recovered. We do so by means of a negative TRPO step applied on the cost of agent i_h:

$$\theta_{k+1}^{i_h} = \theta_k^{i_h} - \alpha^j\sqrt{\frac{2\delta}{\boldsymbol{b}^{i_h T}(\boldsymbol{H}^{i_h})^{-1}\boldsymbol{b}^{i_h}}}\left(\boldsymbol{H}^{i_h}\right)^{-1}\boldsymbol{b}^{i_h}. \tag{12}$$

To put it together, we refer to this algorithm as *MACPO*, and provide its pseudocode in Algorithm 2.

Algorithm 2: MACPO

Input: Stepsize α, batch size B, number of: agents n, episodes K, steps per episode T, possible steps in line search L.
Initialize: Actor networks $\{\theta_0^i,\ \forall i \in \mathcal{N}\}$, Global V-value network $\{\phi_0\}$, Individual V^i-cost networks $\{\phi_{j,0}^i\}_{i=1:n,j=1:m}$, Replay buffer $\mathcal{B}$
for $k = 0, 1, \ldots, K-1$ **do**
  Collect a set of trajectories by running the joint policy $\boldsymbol{\pi}_{\boldsymbol{\theta}_k}$.
  Push transitions $\{(o_t^i, a_t^i, o_{t+1}^i, r_t), \forall i \in \mathcal{N}, t \in T\}$ into $\mathcal{B}$.
  Sample a random minibatch of M transitions from $\mathcal{B}$.
  Compute advantage function $\hat{A}(\mathrm{s}, \mathbf{a})$ based on global V-value network with GAE.
  Compute cost-advantage functions $\hat{A}_j^i(\mathrm{s}, \mathrm{a}^i)$ based on individual V^i-cost critics with GAE.
  Draw a random permutation of agents $i_{1:n}$.
  Set $M^{i_1}(\mathrm{s}, \mathbf{a}) = \hat{A}(\mathrm{s}, \mathbf{a})$.
  for agent $i_h = i_1, \ldots, i_n$ **do**
    Estimate the gradient of the agent's maximisation objective (13).
    for $j = 1, \ldots, m^{i_h}$ **do**
      Estimate the gradient of the agent's j^{th} cost (14).
    end for
    Set $\hat{\boldsymbol{B}}^{i_h} = \left[\hat{\boldsymbol{b}}_1^{i_h}, \ldots, \hat{\boldsymbol{b}}_m^{i_h}\right]$.
    Compute $\hat{\boldsymbol{H}}_k^{i_h}$, the Hessian of the average KL-divergence
    $$\frac{1}{BT}\sum_{b=1}^{B}\sum_{t=1}^{T} D_{\mathrm{KL}}\left(\pi_{\theta_k^{i_h}}^{i_h}(\cdot|o_t^{i_h}), \pi_{\theta^{i_h}}^{i_h}(\cdot|o_t^{i_h})\right).$$
    if the problem is feasible **then**
      Solve the dual (11) for $\lambda_*^{i_h}$, $\mathbf{v}_*^{i_h}$.
      Use the conjugate gradient algorithm to compute the update direction (15).
      Update agent i_h's policy by (16), where $j \in \{0, 1, \ldots, L\}$ is the smallest such j which improves the sample loss, and satisfies the sample constraints, found by the backtracking line search.
    else
      Use equation (12) to recover policy $\theta_{k+1}^{i_h}$ from unfeasible points.
    end if
    Compute (17). //Unless $h = n$.
  end for
  Update V-value network by formula (18).
end for

$$\hat{\boldsymbol{g}}_k^{i_h} = \frac{1}{B}\sum_{b=1}^{B}\sum_{t=1}^{T}\nabla_{\theta_k^{i_h}}\log\pi_{\theta_k^{i_h}}^{i_h}\left(a_t^{i_h}\mid o_t^{i_h}\right)M^{i_{1:h}}(s_t,\boldsymbol{a}_t), \tag{13}$$

$$\hat{\boldsymbol{b}}_j^{i_h} = \frac{1}{B}\sum_{b=1}^{B}\sum_{t=1}^{T}\nabla_{\theta_k^{i_h}}\log\pi_{\theta_k^{i_h}}^{i_h}\left(a_t^{i_h}|o_t^{i_h}\right)\hat{A}_j^{i_h}(s_t,a_t^{i_h}), \tag{14}$$

$$\boldsymbol{x}_k^{i_h} = (\hat{\boldsymbol{H}}_k^{i_h})^{-1}\left(\boldsymbol{g}_k^{i_h} - \hat{\boldsymbol{B}}^{i_h}\mathbf{v}_*^{i_h}\right), \tag{15}$$

$$\theta_{k+1}^{i_h} = \theta_k^{i_h} + \frac{\alpha^j}{\lambda_*^{i_h}}\hat{\boldsymbol{x}}_k^{i_h}, \tag{16}$$

$$M^{i_{1:h+1}}(\mathrm{s},\mathbf{a}) = \frac{\pi_{\theta_{k+1}^{i_h}}^{i_h}\left(\mathrm{a}^{i_h}\mid \mathrm{o}^{i_h}\right)}{\pi_{\theta_k^{i_h}}^{i_h}\left(\mathrm{a}^{i_h}\mid \mathrm{o}^{i_h}\right)}M^{i_{1:h}}(\mathrm{s}_t,\mathbf{a}_t), \tag{17}$$

$$\phi_{k+1} = \arg\min_{\phi}\frac{1}{\mathcal{N}}\frac{1}{T}\sum_{n=1}^{\mathcal{N}}\sum_{t=0}^{T}\left(V_\phi(s_t)-\hat{R}_t\right)^2. \tag{18}$$

4.3. MAPPO-Lagrangian

As an alternative to MACPO, one can use Lagrangian multipliers in place of optimisation with linear and quadratic constraints to solve Equation (9). The Lagrangian method is simple to implement, and it does not require the repetitive computation of the Hessian $\boldsymbol{H}^{i_h}$ whose size grows quadratically with the dimension of the parameter vector θ^{i_h}.

Before we proceed, let us briefly recall the optimisation procedure with a Lagrangian multiplier. Suppose that our goal is to maximise a bounded real-valued function $f(x)$ under a constraint $g(x)$; $\max_x f(x), \text{s.t. } g(x) \leq 0$. We can introduce a scalar variable λ and reformulate the optimisation by

$$\max_x \min_{\lambda\geq 0} f(x) - \lambda g(x). \tag{19}$$

Suppose that x_+ satisfies $g(x_+) > 0$. This immediately implies that $-\lambda g(x_+) \to -\infty$, as $\lambda \to +\infty$, and so Equation (19) equals $-\infty$ for $x = x_+$. On the other hand, if x_- satisfies $g(x_-) \leq 0$, we have that $-\lambda g(x_-) \geq 0$, with equality only for $\lambda = 0$. In that case, the optimisation objective's value equals $f(x_-) > -\infty$. Hence, the only candidate solutions to the problem are those x that satisfy the constraint $g(x) \leq 0$, and the objective matches with $f(x)$.

We can employ the above trick to the constrained optimisation problem from Equation (9) by subsuming the cost constraints into the optimisation objective with Lagrangian multipliers. As such, agent i_h computes $\bar{\lambda}^{i_h}_{1:m^{i_h}}$ and $\theta^{i_h}_{k+1}$ to solve the following min-max optimisation problem

$$\max_{\theta^{i_h}} \min_{\lambda^{i_h}_{1:m^{i_h}} \geq 0} \Bigg[\mathbb{E}_{\mathrm{s}\sim\rho_{\boldsymbol{\pi}_{\boldsymbol{\theta}_k}}, \mathbf{a}^{i_{1:h-1}}\sim\boldsymbol{\pi}^{i_{1:h-1}}_{\boldsymbol{\theta}^{i_{1:h-1}}_{k+1}}, \mathrm{a}^{i_h}\sim\pi^{i_h}_{\theta^{i_h}}} \left[A^{i_h}_{\boldsymbol{\pi}_{\boldsymbol{\theta}_k}} \left(\mathrm{s}, \mathbf{a}^{i_{1:h-1}}, \mathrm{a}^{i_h}\right) \right] - \sum_{u=1}^{m^{i_h}} \lambda^{i_h}_u \left(\mathbb{E}_{\mathrm{s}\sim\rho_{\boldsymbol{\pi}_{\boldsymbol{\theta}_k}}, \mathrm{a}^{i_h}\sim\pi^{i_h}_{\theta^{i_h}}} \left[A^{i_h}_{u,\boldsymbol{\pi}_{\boldsymbol{\theta}_k}} \left(\mathrm{s}, \mathrm{a}^{i_h}\right) \right] + d^{i_h}_u \right) \Bigg],$$
$$\text{s.t. } \overline{D}_{\mathrm{KL}}\left(\pi^{i_h}_{\theta^{i_h}_k}, \pi^{i_h}_{\theta^{i_h}}\right) \leq \delta. \tag{20}$$

Although the objective from Equation (20) is affine in the Lagrangian multipliers $\lambda^{i_h}_u$ $(u = 1, \ldots, m^{i_h})$, which enables gradient-based optimisation, computing the KL-divergence constraint still complicates the overall process. To handle this, one can further simplify it by adopting the *PPO-clip* objective [39], which enables replacing the KL-divergence constraint with the *clip* operator, and update the policy parameter with first-order methods. We do so by defining

$$A^{i_h,(\lambda)}_{\boldsymbol{\pi}_{\boldsymbol{\theta}_k}} \left(s, \boldsymbol{a}^{i_{1:h-1}}, a^{i_h}\right) \triangleq A^{i_h}_{\boldsymbol{\pi}_{\boldsymbol{\theta}_k}} \left(s, \boldsymbol{a}^{i_{1:h-1}}, a^{i_h}\right) - \sum_{u=1}^{m^{i_h}} \lambda^{i_h}_u \left(A^{i_h}_{u,\boldsymbol{\pi}_{\boldsymbol{\theta}_k}} \left(s, a^{i_h}\right) + d^{i_h}_u \right),$$

and rewriting the Equation (20) as

$$\max_{\theta^{i_h}} \min_{\lambda^{i_h}_{1:m^{i_h}} \geq 0} \mathbb{E}_{\mathrm{s}\sim\rho_{\boldsymbol{\pi}_{\boldsymbol{\theta}_k}}, \mathbf{a}^{i_{1:h-1}}\sim\boldsymbol{\pi}^{i_{1:h-1}}_{\boldsymbol{\theta}^{i_{1:h-1}}_{k+1}}, \mathrm{a}^{i_h}\sim\pi^{i_h}_{\theta^{i_h}}} \left[A^{i_h,(\lambda)}_{\boldsymbol{\pi}_{\boldsymbol{\theta}_k}} \left(\mathrm{s}, \mathbf{a}^{i_{1:h-1}}, \mathrm{a}^{i_h}\right) \right],$$
$$\text{s.t. } \overline{D}_{\mathrm{KL}}\left(\pi^{i_h}_{\theta^{i_h}_k}, \pi^{i_h}_{\theta^{i_h}}\right) \leq \delta. \tag{21}$$

The objective in Equation (21) takes a form of an expectation with a KL-divergence constraint on the policy. Up to the error of approximation of

KL-constraint with the *clip* operator, it can be equivalently transformed into an optimisation of a clipping objective. Finally, the objective takes the form

$$\mathbb{E}_{\mathrm{s}\sim\rho_{\boldsymbol{\pi}_{\boldsymbol{\theta}_k}},\mathbf{a}^{i_{1:h-1}}\sim\boldsymbol{\pi}^{i_{1:h-1}}_{\boldsymbol{\theta}^{i_{1:h-1}}_{k+1}},\mathrm{a}^{i_h}\sim\pi^{i_h}_{\theta^{i_h}_k}}\Bigg[\min\Bigg(\frac{\pi^{i_h}_{\theta^{i_h}}(\mathrm{a}^{i_h}|\mathrm{s})}{\pi^{i_h}_{\theta^{i_h}_k}(\mathrm{a}^{i_h}|\mathrm{s})}A^{i_h,(\lambda)}_{\boldsymbol{\pi}_{\boldsymbol{\theta}_k}}\left(\mathrm{s},\mathbf{a}^{i_{1:h-1}},\mathrm{a}^{i_h}\right),$$
$$\mathrm{clip}\Bigg(\frac{\pi^{i_h}_{\theta^{i_h}}(\mathrm{a}^{i_h}|\mathrm{s})}{\pi^{i_h}_{\theta^{i_h}_k}(\mathrm{a}^{i_h}|\mathrm{s})},1\pm\epsilon\Bigg)A^{i_h,(\lambda)}_{\boldsymbol{\pi}_{\boldsymbol{\theta}_k}}\left(\mathrm{s},\mathbf{a}^{i_{1:h-1}},\mathrm{a}^{i_h}\right)\Bigg)\Bigg]. \tag{22}$$

The clip operator replaces the policy ratio with $1-\epsilon$, or $1+\epsilon$, depending on whether its value is below or above the threshold interval. As such, agent i_h can learn within its trust region by updating θ^{i_h} to maximise Equation (22), while the Lagrangian multipliers are updated towards the direction opposite to their gradients of Equation (20), which can be computed analytically. We name this algorithm *MAPPO-Lagrangian*, and give its pseudocode in Algorithm 3.

$$M^{i_h,(\lambda)}(\mathrm{s}_t,\mathbf{a}_t)=M^{i_h}(\mathrm{s}_t,\mathbf{a}_t)-\sum_{j=1}^{n}\lambda^{i_h}_j\hat{A}^{i_h}_j(\mathrm{s}_t,\mathrm{a}^{i_h}_t), \tag{23}$$

$$\Delta_{\theta^{i_h}}=\nabla_{\theta^{i_h}}\frac{1}{B}\sum_{b=1}^{B}\sum_{t=0}^{T}\min\Bigg(\frac{\pi^{i_h}_{\theta^{i_h}}\left(a^{i_h}_t\mid o^{i_h}_t\right)}{\pi^{i_h}_{\theta^{i_h}_k}\left(a^{i_h}_t\mid o^{i_h}_t\right)}M^{i_h,(\lambda)}(s_t,\boldsymbol{a}_t),$$
$$\mathrm{clip}\Bigg(\frac{\pi^{i_h}_{\theta^{i_h}}\left(a^{i_h}_t\mid o^{i_h}_t\right)}{\pi^{i_h}_{\theta^{i_h}_k}\left(a^{i_h}_t\mid o^{i_h}_t\right)},1\pm\epsilon\Bigg)M^{i_h,(\lambda)}(s_t,\boldsymbol{a}_t)\Bigg), \tag{24}$$

$$d^{i_h}_j=\frac{1}{BT}\sum_{b=1}^{B}\sum_{t=1}^{T}\hat{V}^{i_h}_j(s_t)-C^{i_h}_j, \tag{25}$$

Algorithm 3: MAPPO-Lagrangian

Input: Stepsizes $\alpha_\theta, \alpha_\lambda$, batch size B, number of: agents n, episodes K, steps per episode T, discount factor γ.
Initialize: Actor networks $\{\theta_0^i,\ \forall i \in \mathcal{N}\}$, Global V-value network $\{\phi_0\}$, V-cost networks $\{\phi_{j,0}^i\}_{1\le j\le m^i}^{i\in\mathcal{N}}$, Replay buffer $\mathcal{B}$.
for $k = 0, 1, \ldots, K-1$ **do**
  Collect a set of trajectories by running the joint policy $\boldsymbol{\pi}_{\boldsymbol{\theta}_k}$.
  Push transitions $\{(o_t^i, a_t^i, o_{t+1}^i, r_t), \forall i \in \mathcal{N}, t \in T\}$ into $\mathcal{B}$.
  Sample a random minibatch of B transitions from $\mathcal{B}$.
  Compute advantage function $\hat{A}(\mathrm{s}, \mathbf{a})$ based on global V-value network with GAE.
  Compute cost advantage functions $\hat{A}_j^i(\mathrm{s}, \mathrm{a}^i)$ for all agents and costs, based on V-cost networks with GAE.
  Draw a random permutation of agents $i_{1:n}$.
  Set $M^{i_1}(\mathrm{s}, \mathbf{a}) = \hat{A}(\mathrm{s}, \mathbf{a})$.
  for agent $i_h = i_1, \ldots, i_n$ **do**
    Initialise a policy parameter $\theta^{i_h} = \theta_k^{i_h}$,
    and Lagrangian multipliers $\lambda_j^{i_h} = 0$, $\forall j = 1, \ldots, m^{i_h}$.
    Compute the Lagrangian in Equation (23).
    for $e = 1, \ldots, e_{\mathrm{PPO}}$ **do**
      Compute the gradient $\Delta_{\theta^{i_h}}$ of the Lagrangian PPO-Clip objective with Equation (24).
      Update temprorarily the actor paramaters
      $$\theta^{i_h} \leftarrow \theta^{i_h} + \alpha_\theta \Delta_{\theta^{i_h}}.$$
      for $j = 1, \ldots, m^{i_h}$ **do**
        Approximate the constraint violation via Equation (25).
        Differentiate the constraint via Equation (26).
      end for
      for $j = 1, \ldots, m^{i_h}$ **do**
        Update temporarily the Lagrangian multiplier as in Equation (27).
      end for
    end for
    Update the actor parameter $\theta_{k+1}^{i_h} = \theta^{i_h}$.
    Compute Equation (28). //Unless $h = n$.
  end for
  Update the critic via Equation (29).
end for

$$\Delta\lambda_j^{i_h} = \frac{-1}{B}\sum_{b=1}^{B}\left(d_j^{i_h}(1-\gamma) + \sum_{t=0}^{T}\frac{\pi_{\theta^{i_h}}^{i_h}(a_t^{i_h}|o_t^{i_h})}{\pi_{\theta_k^{i_h}}^{i_h}(a_t^{i_h}|o_t^{i_h})}\hat{A}_j^{i_h}(s_t, a_t^{i_h})\right), \tag{26}$$

$$\lambda_j^{i_h} \leftarrow \mathrm{ReLU}\left(\lambda_j^{i_h} - \alpha_\lambda \Delta\lambda_j^{i_h}\right), \tag{27}$$

$$M^{i_{h+1}}(\mathrm{s}, \mathbf{a}) = \frac{\pi_{\theta_{k+1}^{i_h}}^{i_h}\left(\mathrm{a}^{i_h} \mid \mathrm{o}^{i_h}\right)}{\pi_{\theta_k^{i_h}}^{i_h}\left(\mathrm{a}^{i_h} \mid \mathrm{o}^{i_h}\right)} M^{i_h}(\mathrm{s}, \mathbf{a}), \tag{28}$$

$$\phi_{k+1} = \arg\min_{\phi} \frac{1}{BT}\sum_{b=1}^{B}\sum_{t=0}^{T}\left(V_\phi(s_t) - \hat{R}_t\right)^2. \tag{29}$$

5. Experiments

In this section, first, we introduce three safe MARL benchmarks. Second, we provide and analyse results of experiments conducted in these environments. Lastly, for completeness, we give the details of settings for the experiments at the end of the section.

5.1. Safe Multi-Agent MuJoCo

Although MARL researchers have long had a variety of environments to test different algorithms, such as StarCraftII [37] and Multi-Agent MuJoCo [32], no public safe MARL benchmark has been proposed; this impedes researchers from evaluating and benchmarking safety-aware multi-agent learning methods. As a key contribution of this paper, we introduce three Safe MARL benchmarks, Safe MAMuJoCo, Safe MARobosuite and Safe MAIG. We use these environments to evaluate the performance of our methods, in terms of reward and safety, against strong baselines.

5.1.1. Safe Multi-Agent MuJoCo: the Environment

For visualisation see Figure 1. Safe MAMuJoCo is an extension of MA-MuJoCo [32]. In particular, the background environment, agents, physics simulator, and the reward function are preserved. However, as oppose to its predecessor, Safe MAMuJoCo environments come with obstacles, like walls or bombs. Furthermore, with the increasing risk of an agent stumbling upon an obstacle, the environment emits cost [8]. According to the scheme from [44], we characterise the cost functions for each task below.

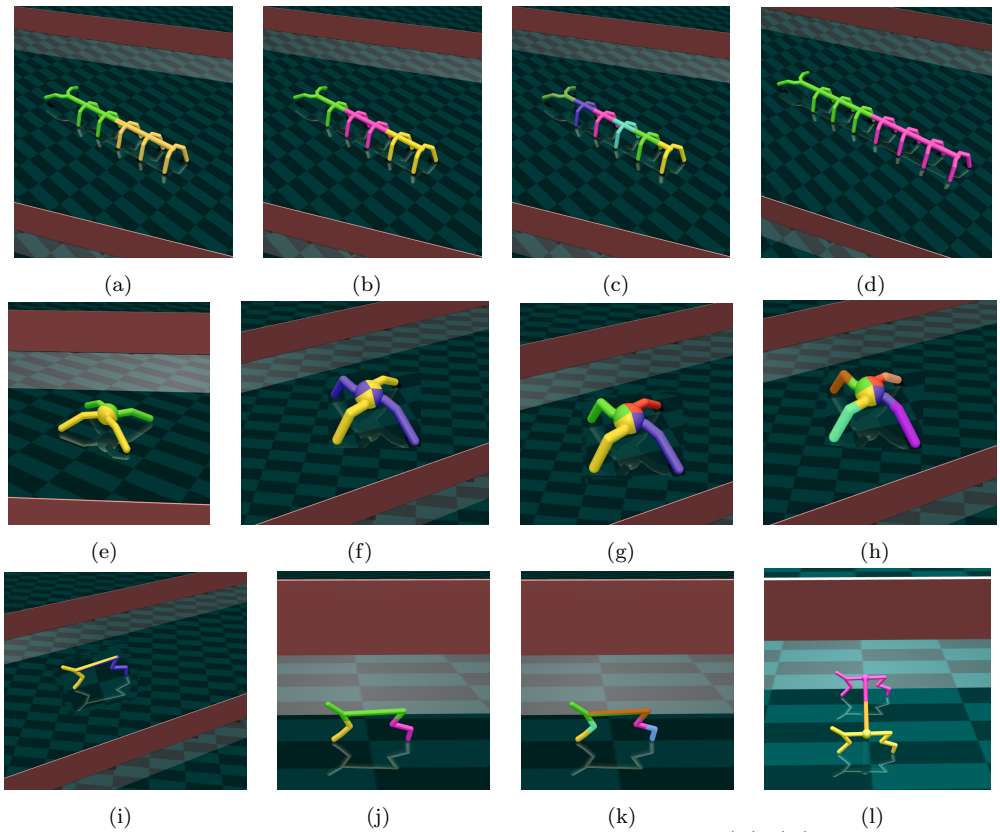

Figure 1: Example tasks in Safe Multi-Agent MuJoCo. (a)-(d): Safe ManyAgent Ant, (e)-(h): Safe Ant, (i)-(l): Safe HalfCheetah. Body parts of different colours are controlled by different agents. Agents jointly learn to manipulate the robot, while avoiding crashing into unsafe red areas.

ManyAgent Ant Task 1.0 & Ant Task 1.0

The width of the corridor set by two walls is 9 m(ManyAgent Ant with 2 agents (2x3), 3 agents (3x2), 6 agents (6x1))/10 m (Ant with 2 (2x4, 2x4d),

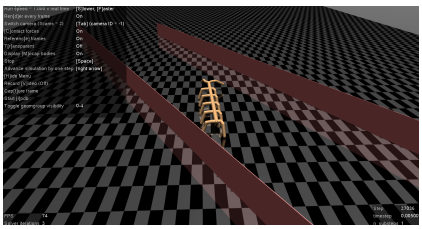

(a) ManyAgent Ant Task 1.0

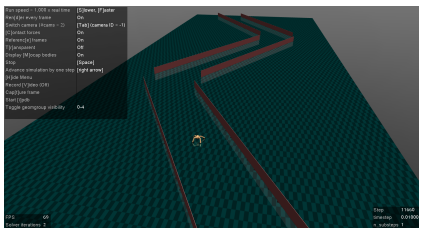

(b) Ant Task 1.0

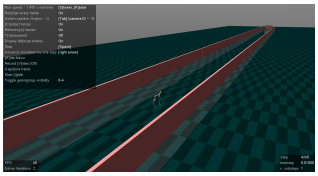

(c) HalfCheetah Task 1.0

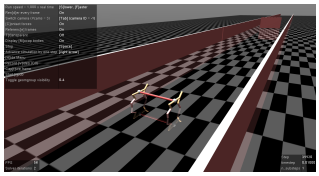

(d) Couple HalfCheetah Task 1.0

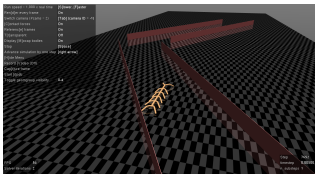

(e) ManyAgent Ant Task 2.1

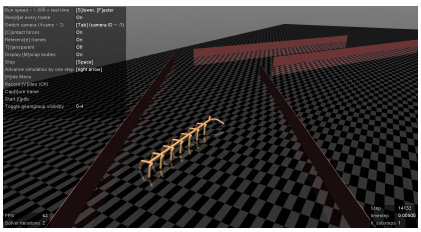

(f) ManyAgent Ant Task 2.2

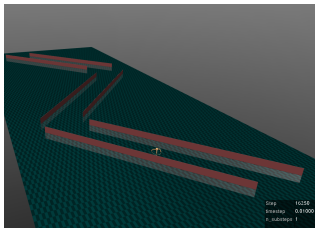

(g) Ant Task 2.1

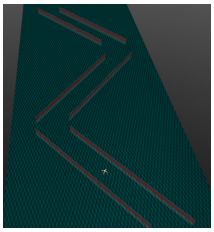

(h) Ant Task 2.2

Figure 2: Specific tasks in Safe Multi-Agent MuJoCo Environment. (a): ManyAgent Ant Task 1.0: ManyAgent Ant 3x2 two folding line walls (corridor width is 9 m). (b): Ant Task 1.0: Ant 4x2 with three folding Jagged (30°) line walls. (c): HalfCheetah Task 1.0: HalfCheetah 2x3 with moving obstacle, (d): Couple HalfCheetah Task 1.0: Couple HalfCheetah 1P1 with moving obstacle, (e): ManyAgent Ant Task 2.1: Many-Agent Ant 3x2 with two folding line walls (corridor width is 12 m). (f): ManyAgent Ant Task 2.2: Many-Agent Ant 4x2 with two folding line walls. (g): Ant Task 2.1: Ant 4x2 with three folding Jagged (40°) line walls (corridor width is 8 m). (g): Ant Task 2.2: Ant 4x2 with three folding Jagged (40°) line walls (corridor width is 10 m).

4 (4x2), 8 (8x1) agents). The environment emits the cost of 1 for an agent, if the distance between the robot and the wall is less than 1.8 m, or when the robot topples over, see Figure 2 (a) and (b). This can be described as

$$\mathrm{c}_t = \begin{cases} 0, & \text{for} \quad 0.2 \leq \boldsymbol{z}_{\text{torso},t+1} \leq 1.0 \text{ and } \left\| \boldsymbol{x}_{\text{torso},t+1} - \boldsymbol{x}_{\text{wall}} \right\|_2 \geq 1.8 \\ 1, & \text{otherwise.} \end{cases}$$

where $\boldsymbol{z}_{\text{torso},t+1}$ is the robot's torso's z-coordinate, and $\boldsymbol{x}_{\text{torso},t+1}$ is the robot's torso's x-coordinate, at time $t+1$; $\boldsymbol{x}_{\text{wall}}$ is the x-coordinate of the wall. A similar cost scheme is implemented in *ManyAgent And Tasks 2.1 & 2.2* and in *Ant Tasks 2.1 & 2.2*.

HalfCheetah Task 1.0 & Couple HalfCheetah Task 1.0

In these tasks, the HalfCheetah agents move inside a corridor (which constraints their movement, but does not induce costs). Together with them, there are bombs moving inside the corridor. If an agent finds itself too close to a bomb, the distance between an agent and a bomb is less than 9 m, a cost of 1 will be emitted, see Figure 2 (c) and (d).

$$\mathrm{c}_t = \begin{cases} 0, & \text{for} \quad \left\| \boldsymbol{y}_{\text{torso},t+1} - \boldsymbol{y}_{\text{obstacle}} \right\|_2 \geq 9 \\ 1, & \text{otherwise.} \end{cases}$$

where $\boldsymbol{y}_{\text{torso},t+1}$ is the y-coordinate of the robot's torso, and $\boldsymbol{y}_{\text{obstacle}}$ is the y-coordinate of the moving obstacle.

5.1.2. Safe Multi-Agent MuJoCo: Experiments

In this section, we use Safe MAMuJoCo to examine if the MACPO/MAPPO-Lagrangian agents can satisfy their safety constraints and cooperatively learn to achieve high rewards, compared to existing MARL algorithms. Notably, our proposed methods adopt two different approaches for achieving safety. MACPO reaches safety via *hard* constraints and backtracking line search, while MAPPO-Lagrangian maintains a rather *soft* safety awareness by performing gradient descent-ascent on the PPO-clip objective.

Figures 3-8 show cost and reward performance comparisons between MACPO, MAPPO-Lagrangian, MAPPO [43], IPPO [16], and HAPPO [21] algorithms on challgenging Safe MAMuJoCo tasks. These figures should be interpreted at three-folds; each subfigure represents a different robot, within each subfigure, three task setups in terms of multi-agent control are considered, and

for each task we plot the cost curves (the lower the better) in the upper row and the reward curves (the higher the better) in the bottom row.

The experiments reveal that both MACPO and MAPPO-Lagrangian quickly learn to satisfy safety constraints, and keep their explorations within the feasible policy space. This stands in contrast to IPPO, MAPPO, and HAPPO which largely violate the constraints thus being unsafe. Furthermore, our algorithms achieve comparable reward scores; both methods are often better than IPPO. In general, the performance (in terms of reward) of MAPPO-Lagrangian is better than of MACPO; moreover, MAPPO-Lagrangian outperforms the unconstrained MAPPO on challenging *Ant* tasks (Figure 4). We note that on none of the tasks the reward of HAPPO was exceeded, though the algorithm is unsafe.

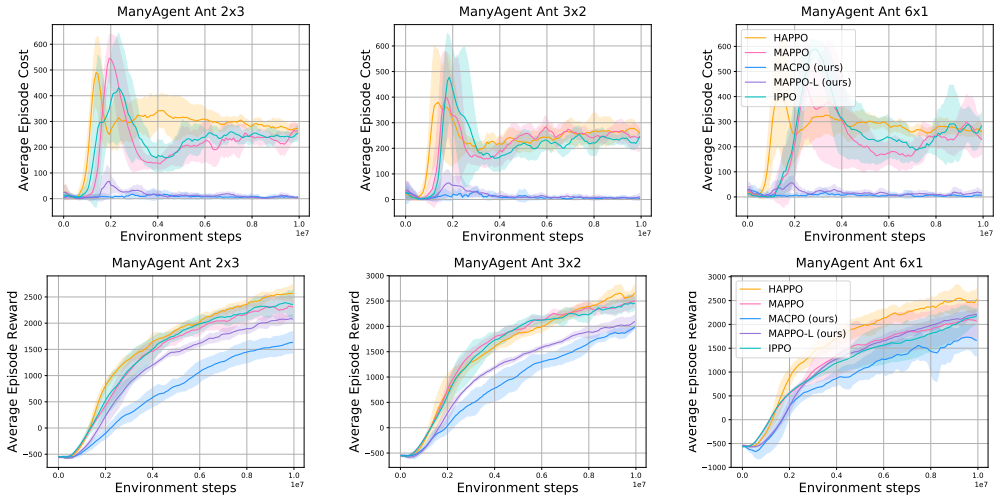

Figure 3: Performance comparisons on Safe ManyAgent Ant task **1.0** in terms of cost (the first row) and reward (the second row). The safety constraint value is 1.

5.2. Safe Multi-Agent Robosuite

In this subsection we describe the Safe Multi-Agent Robosuite environment and provide the results of our experiments conducted on it.

5.2.1. Safe Multi-Agent Robosuite: the Environment

Safe Multi-Agent Robosuite is an extension of Robosuite [47]. We split the control over a robot across multiple controllers of its joints—one or more

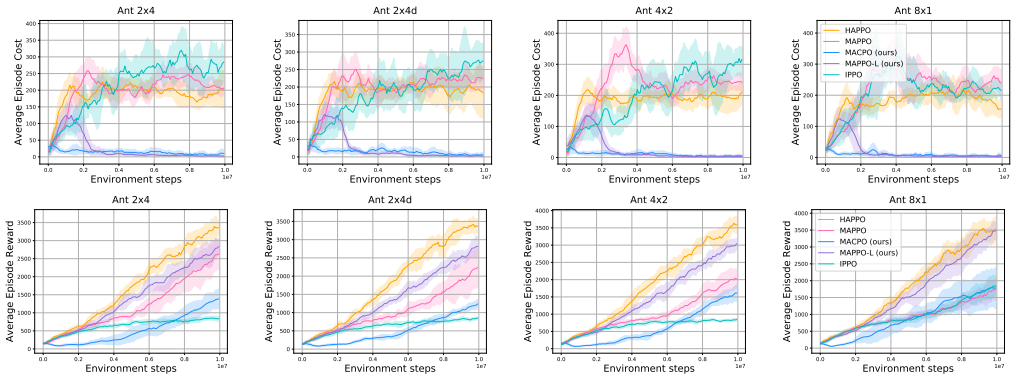

Figure 4: Performance comparisons on Safe Ant task **1.0** in terms of cost (the first row) and reward (the second row). The safety constraint values are: 0.2 for 2-agent and 4-agent Ants, and 1 for 8-agent Ants.

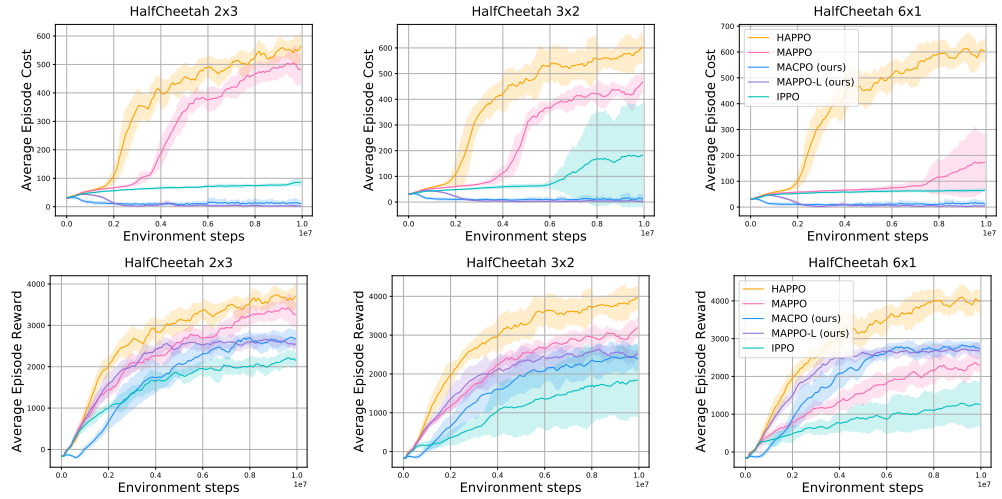

Figure 5: Performance comparisons on tasks of Safe HalfCheetah task **1.0** in terms of cost (the first row) and reward (the second row). The safety constraint value is 5.

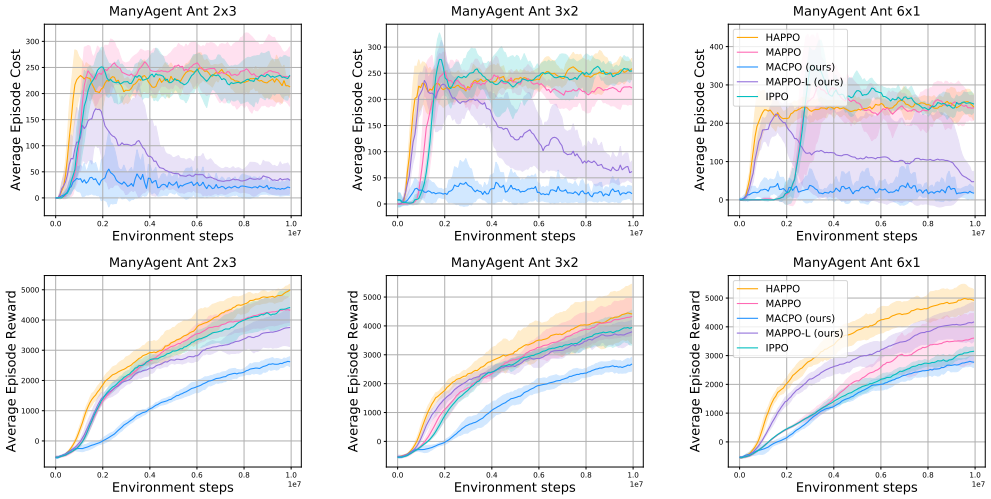

Figure 6: Performance comparisons on Safe ManyAgent Ant task **2.1** in terms of cost (the first row) and reward (the second row). The safety constraint value is set to 10.

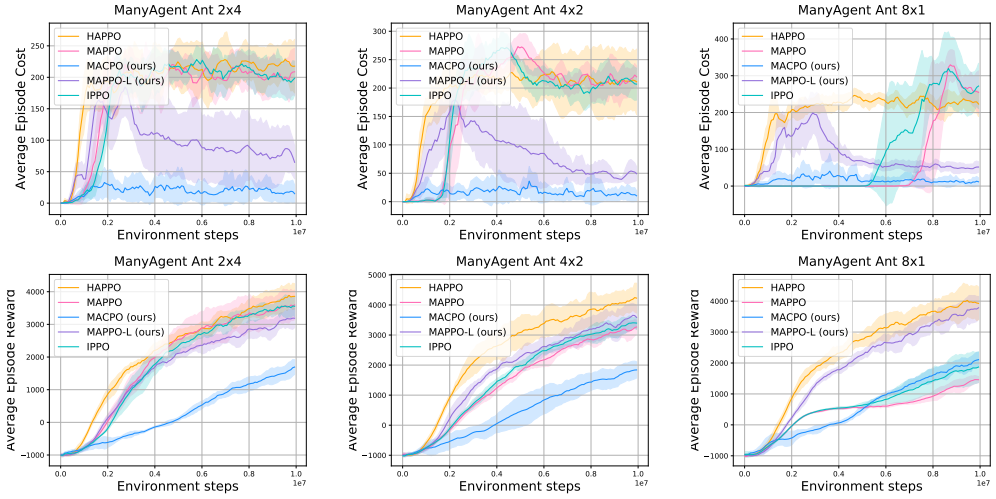

Figure 7: Performance comparisons on Safe ManyAgent Ant task **2.2** in terms of cost (the first row) and reward (the second row). The safety constraint value is set to 10.

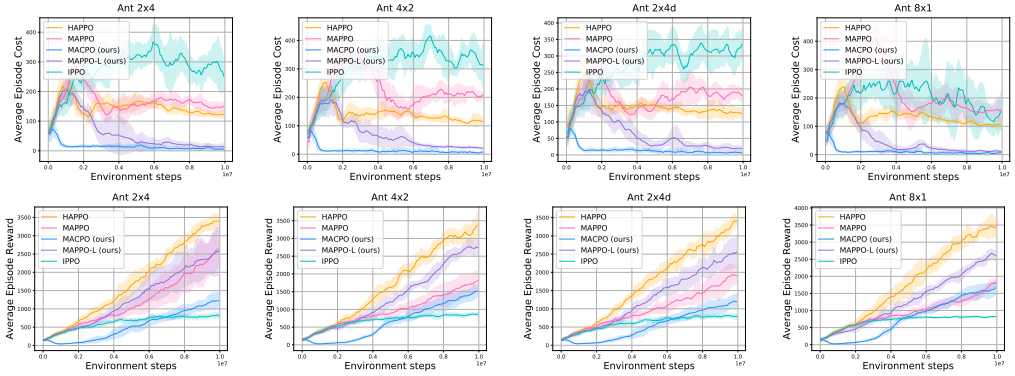

Figure 8: Performance comparisons on Safe Ant task **2.1** in terms of cost (the first row) and reward (the second row). The safety constraint value is 1.

per controller. For example, the *Lift* task comes with 3 variants: 2 four-dimensional agents (2x4 Lift), 4 two-dimensional agents (4x2 Lift), and 8 one-dimensional agents (8x1 Lift).

Safe MARobosuite tasks are fully cooperative, partialy observable, continuous, and safety-aware. Its multi-agency makes it a compatible framework for training modular robots which are built of multiple, robust parts [3]. We adopt the reward setting from Robosuite and present it below.

Lift & Stack

The task is to grasp and lift a blue object from a table up to at least 0.1m of height. At the same time, to assure safety, we require that the robotic gripper avoids physical contact with the table, *i.e.*, keeps at least 0.02m distance from it (see Equation (30)). For visualisation, see Figure 9,

$$\mathrm{c}_t = \begin{cases} 1.0, & \text{for} \quad |\boldsymbol{p}_{\text{eef},t+1} - \boldsymbol{z}_{\text{obstacle}}| \leq 0.02 \\ 0, & \text{otherwise.} \end{cases} \tag{30}$$

where $\boldsymbol{p}_{\text{eef},t+1}$ is the z-coordinate of the robot's end gripper , and $\boldsymbol{z}_{\text{obstacle}}$ is the z-coordinate of the obstacle.

TwoArmPegInHole

The agents learn to insert a peg into a hole of a rim. Additionally, the agents are required to keep the peg at at least 0.11m distance from a red part of the rim (see Equation (31) for cost and Figure 9 for visualisation).

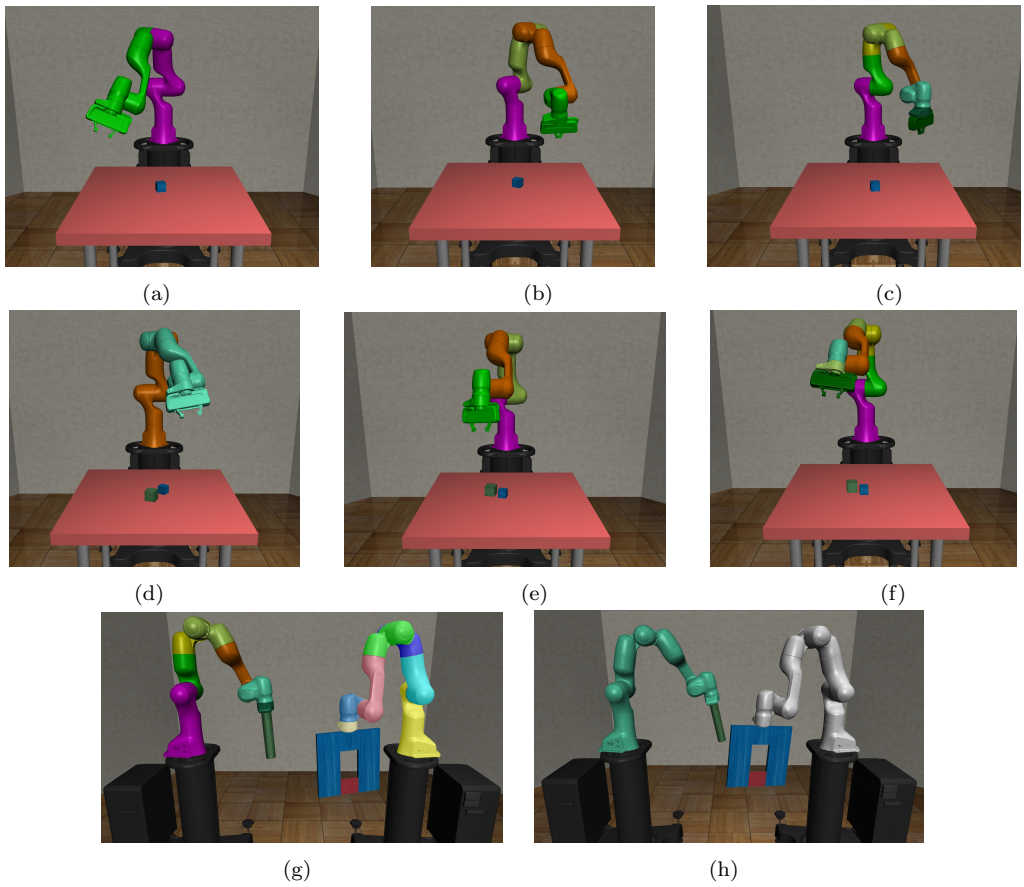

Figure 9: Example tasks in Safe MARobosuite Environment. (a): Safe 2x4-Lift, (b): Safe 4x2-Lift, (c): Safe 8x1-Lift, (d): Safe 2x4-Stack, (e): Safe 4x2-Stack, (f): Safe 8x1-Stack, (g): Safe 14x1-TwoArmPegInHole, (h): Safe 2x7-TwoArmPegInHole. Body parts of different colours of robots are controlled by different agents. Agents jointly learn to manipulate the robot, while avoiding crashing into unsafe red areas.

$$\mathrm{c}_t = \begin{cases} 1.0, & \text{for} \quad \boldsymbol{p}_{\mathrm{pd},t+1} \leq -0.11 \\ 0, & \text{otherwise.} \end{cases} \tag{31}$$

where $\boldsymbol{p}_{\mathrm{pd},t+1}$ is the parallel distance between the robot's peg and robot's hole centre.

5.2.2. Safe Multi-Agent Robosuite: Experiments

We study the performance of our methods in Safe TwoArmPegInHole in comparison to the aforementioned baselines. Notably, from Figure 10 we learn that IPPO completely fails to increase reward in TwoArmPegInHole 2x7, which suggests that the environment's difficulty is higher than that of Safe MAMuJoCo.

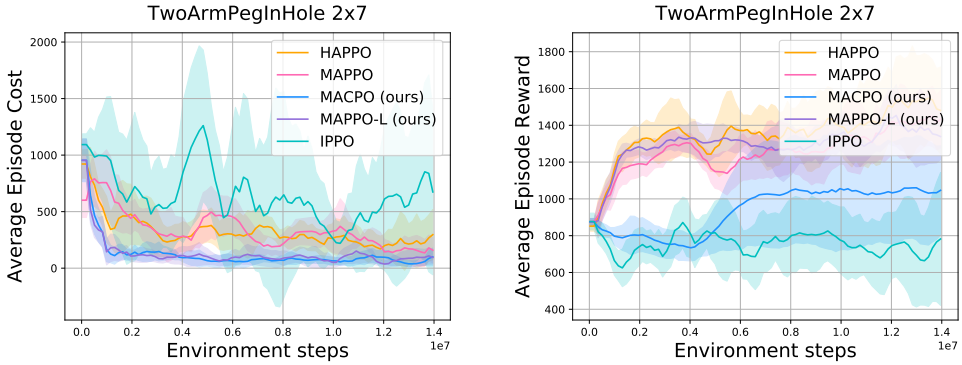

Figure 10: Performance comparisons on Safe TwoArmPegInHole 2x7 task, with the safety constraint set to 30.

5.3. Safe Multi-Agent Isaac Gym

Safe Multi-Agent Isaac Gym (Safe MAIG) is developed on top of Isaac Gym [29]—a high performance, GPU-based platform for robotics tasks that utilises the Nvidia PhysX [31] engine. Again, we employ this environment to compare our methods to other MARL algorithms.

5.3.1. Safe Multi-Agent Isaac Gym: the Environment

In this section we describe our tasks: ShadowHandOver (2x6, 6x2, 4x3, 12x1), ShadowHandCatchUnderarm (2x6, 6x2, 12x1), and ShadowHandReOrientation (2x6, 6x2, 12x1), in detail and visualise them in Figure 11.

ShadowHandOver (2x6, 6x2, 4x3, 12x1)

The environment involves two hands at fixed positions. The first hand with an object must find a way to hand the item over to the second hand, while one finger on the first hand has safety constraints (see Figure 11) over the range of motion of one of the fingers. Formally, the cost is given by

$$\mathrm{c}_t = \begin{cases} 1.0, & \text{for} \quad |\boldsymbol{F}_{\mathrm{a}4,t+1}| \geq 0.1 \\ 0, & \text{otherwise,} \end{cases}$$

where $\boldsymbol{F}_{\mathrm{a}4,t+1}$ is the first hand's fourth fingers's motion degree.

ShadowHandCatchUnderarm (2x6, 6x2, 4x3, 12x1)

This task is an extension of ShadowHandOver in which the hands can move freely, *i.e.*, they can translate/rotate their centres of masses within some region (see Figure 11). The safety constraints are as in the previous task.

ShadowHandReOrientation (2x6, 6x2, 4x3, 12x1)

In each of two hands there are two items. The goal of the agents is to rotate the two items around each other (see Figure 11). The safety constraints remain the same.

5.3.2. Safe Multi-Agent Isaac Gym: Experiments

Again, the study reveals that the performance of our methods in terms of reward is competitive with the SOTA MARL methods, meanwhile being safe. Furthermore, as Figures 12-13 show, MACPO learns to meet the safety constraints faster than MAPPO-Lagrangian. The latter algorithm, however, performs better in terms of reward.

5.4. Sensitivity Analysis for Safety-Bound-Parameters Tuning

We analyse the sensitivity of MACPO to changes in the size of safety bound (*bound c*) on Figure 14. We learn that with that the algorithm's *effectiveness* does not change under different safety levels. However, with the stricter safety constraints, the reward performance of MACPO decreases.

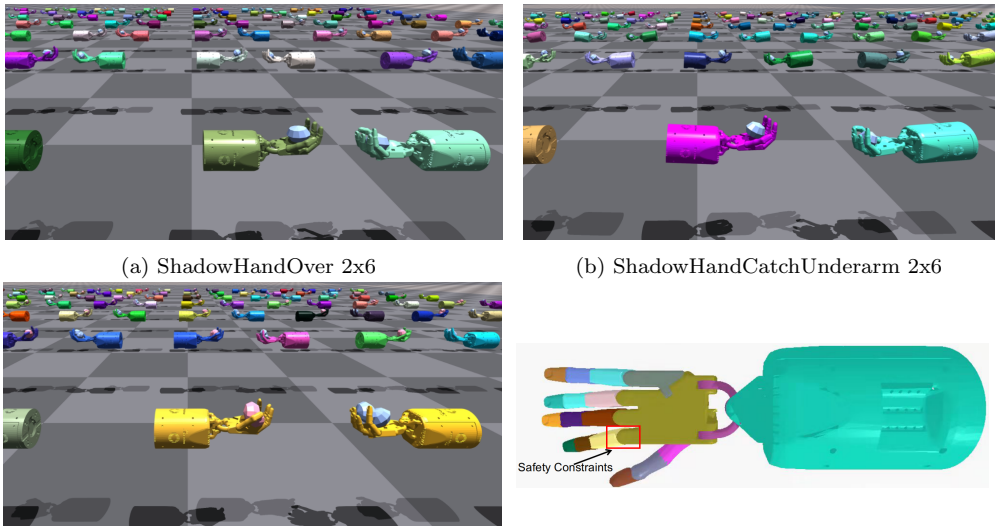

(a) ShadowHandOver 2x6

(b) ShadowHandCatchUnderarm 2x6

(c) ShadowHandReOrientation 4x3

(d) A hand showing safety constraints

Figure 11: Safe multi-agent Isaac Gym environments. Body parts of different colours of robots are controlled by different agents in each pair of hands. Agents jointly learn to manipulate the robot, while avoiding violating the safety constraints.

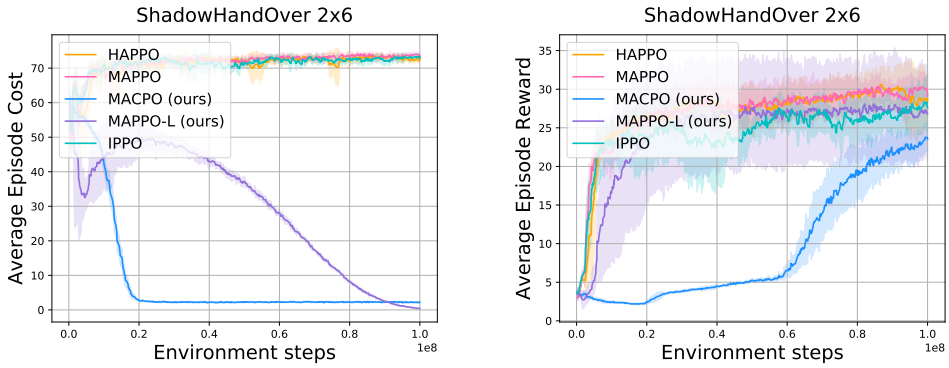

Figure 12: ShadowHandOver 2x6 task: performance comparisons Safe ShadowHandOver 2x6 task in terms of cost and reward, the safety constraint value is set to 2.5. Our algorithms are the only ones that learn the safety constraints, while achieving satisfying performance in terms of the reward.

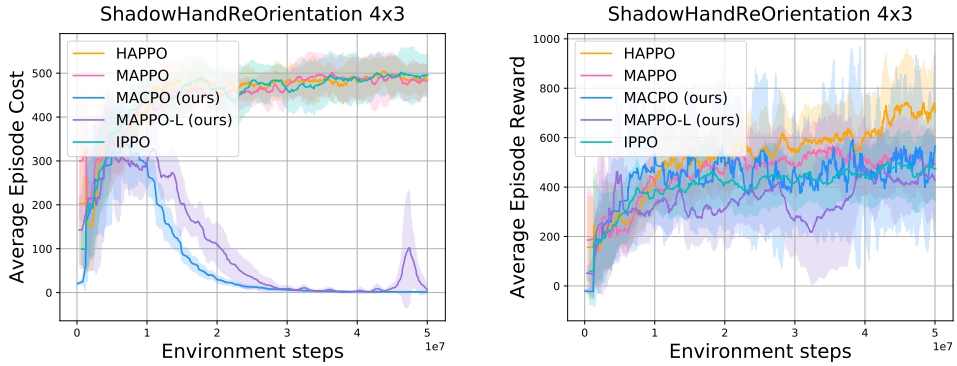

Figure 13: ShadowHandReOrientation 4x3 task: performance comparisons on Safe ShadowHandReOrientation 4x3 task in terms of cost and reward. The safety constraint value is set to 0.1.

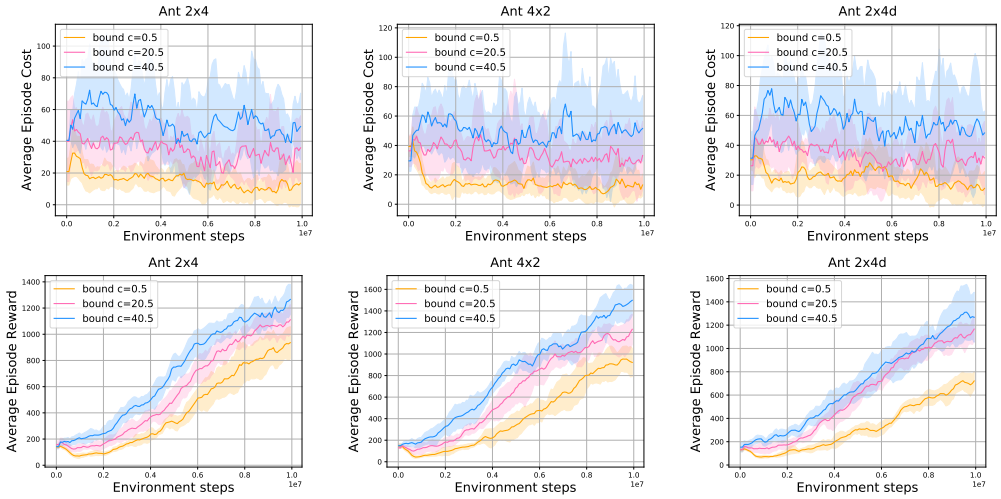

Figure 14: Ant 2x4, 4x2, 2x4d tasks **2.2**, MACPO with different safety bound in terms of costs and rewards.

6. Conclusion

In this paper, we have made a step towards solving multi-robot control problems with safety constraints via safe multi-agent reinforcement learning. We introduced the first general formulation of the safe MARL problem and analysed it theoretically. Central to our findings is a safe multi-agent policy iteration procedure that attains theoretically-justified monotonic improvement and constraints satisfaction guarantee at every iteration. As further outcomes to our analysis, we proposed two practical algorithms: MACPO and MAPPO-Lagrangian. To demonstrate their effectiveness, as well as to increase the range of testbeds for Safe MARL methods, we introduced three new benchmark suites of Safe MAMuJoCo, Safe MARobosuite and Safe MAIG. We used them to compare our methods against strong MARL baselines, over which they showed a significant advantage in terms of safety, and comparable performance in terms of the reward. We believe that our findings will contribute to the rise and applicability of many safe MARL methods for multi-robot control.

Acknowledgments

This work was partially supported by the European Union's Horizon 2020 Framework Programme for Research and Innovation under the Specific Grant Agreement No. 945539 (Human Brain Project SGA3). We would like to thank Hengrui Zhang for his help to run some of experiments.

Appendix A. Details of Settings for Experiments

In this section, we provide the details of settings for our experiments. The code is available at:
https://sites.google.com/view/aij-safe-marl/.

hyperparameters	value	hyperparameters	value
gain	0.01	optimizer	Adam
activation	ReLU	optim eps	1e-5
std x coef	1	max grad norm	10
std y coef	0.5	actor network	mlp

Table A.1: In the Safe MAMuJoCo, Safe MARobosuite and Safe MAIG domains, common hyperparameters used for MAPPO-Lagrangian, MAPPO, HAPPO, IPPO, and MACPO.

hyperparameters	value	hyperparameters	value
critic lr	5e-3	hidden layer	1
gamma	0.99	eval episodes	32
hidden layer dim	64	episode length	[1000, 2000]
num mini-batch	40	batch size	16000
training threads	4	rollout threads	16

Table A.2: In the Safe MAMuJoCo and Safe MARobosuite domains, common hyperparameters used for MAPPO-Lagrangian, MAPPO, HAPPO, IPPO, and MACPO (episode length: 1000 used for Safe MAMuJoCo, 2000 used for Safe MARobosuite).

hyperparameters	value	hyperparameters	value
critic lr	[1e-3^a, 5e-4^b]	hidden layer	2
gamma	0.96	episode length	8
training env number	[512^a, 2048^b]	eval episodes	10000
rollout threads	80	hidden layer dim	512
num mini-batch	1	num env steps	[100 m^a, 50 m^b]

Table A.3: In the Safe MAIG domains, common hyperparameters used for MAPPO-Lagrangian, MAPPO, HAPPO, IPPO, and MACPO (m denotes million, a indicates the parameter is used for ShadowHandOver task, b indicates the parameter is used for ShadowHandReOrientation task).

Algorithms	MAPPO-L	MAPPO	HAPPO	IPPO	MACPO
ppo epoch	5	5	5	5	/
ppo-clip	0.2	0.2	0.2	0.2	/
Lagrangian lr	1e-3	/	/	/	/
fraction	/	/	/	/	0.5

Table A.4: In the Safe MAMuJoCo, Safe MARobosuite and Safe MAIG domains, different hyperparameters used for MAPPO-Lagrangian, MAPPO, HAPPO, IPPO, and MACPO.

Algorithms	MAPPO-L	MAPPO	HAPPO	IPPO	MACPO
actor lr	9e-5	9e-5	9e-5	9e-5	/
kl-threshold	/	/	/	/	[0.0065, 1e-3]
Lagrangian lr	1e-3	/	/	/	/
fraction coef	/	/	/	/	0.27

Table A.5: In the Safe MAMuJoCo and Safe MARobosuite domains, different hyperparameters used for MAPPO-Lagrangian, MAPPO, HAPPO, IPPO, and MACPO (kl-threshold: 0.0065 used for Safe MAMuJoCo, 1e-3 used for Safe MARobosuite).

Parameters	actor lr	kl-threshold	fraction coef
MAPPO-L	[3e-5^a, 5e-4^b]	/	/
MAPPO	[3e-5^a, 5e-4^b]	/	/
HAPPO	[3e-5^a, 5e-4^b]	/	/
IPPO	[3e-5^a, 5e-4^b]	/	/
MACPO	/	[67e-4^a, 65e-4^b]	[0.29^a, 0.27^b]

Table A.6: In the Safe MAIG domains, different hyperparameters used for MAPPO-Lagrangian, MAPPO, HAPPO, IPPO, and MACPO, a indicates the parameter is used for ShadowHandOver task, b indicates the parameter is used for ShadowHandReOrientation task.

task	value	task	value
Ant(2x4) 1.0	0.2	Ant(4x2) 1.0	0.2
Ant(2x4d) 1.0	0.2	HalfCheetah(2x3) 1.0	5
HalfCheetah(3x2) 1.0	5	HalfCheetah(6x1) 1.0	5
ManyAgent Ant(2x3) 1.0	1	ManyAgent Ant(3x2) 1.0	1
ManyAgent Ant(6x1) 1.0	1	TWoArmPegInHole(2x7) 1.0	30
ManyAgent Ant(2x3) 2.1	10	ManyAgent Ant(3x2) 2.1	10
ManyAgent Ant(6x1) 2.1	10	ManyAgent Ant(2x3) 2.2	10
ManyAgent Ant(3x2) 2.2	10	ManyAgent Ant(6x1) 2.2	10
Ant(2x4) 2.1	1	Ant(4x2) 2.1	1
Ant(2x4d) 2.1	1	Ant(8x1) 2.1	1
ShadowHandOver(2x6)	2.5	ShadowHandReOrientation(4x3)	0.1

Table A.7: Safety bound used for MACPO in the Safe MAMuJoCo, Safe MARobosuite Safe MAIG domains.

Appendix B. Solution to the Constrained Optimisation Problem in MACPO

Theorem 2. *The solution to the following problem*

$$\begin{aligned} \boldsymbol{p}* = \min_{x} \boldsymbol{g}^T \boldsymbol{x} \\ s.t.\ \boldsymbol{b}^T \boldsymbol{x} + c \leq 0 \\ \boldsymbol{x}^T \boldsymbol{H} \boldsymbol{x} \leq \delta, \end{aligned}$$

where $\boldsymbol{g}, \boldsymbol{b}, \boldsymbol{x} \in \mathbb{R}^n, c, \delta \in \mathbb{R}, \delta > 0, \boldsymbol{H} \in \mathbb{S}^n$, *and* $\boldsymbol{H} \succ 0$. *When there is at least one strictly feasible point, the optimal point* $\boldsymbol{x}^*$ *satisfies:*

$$\boldsymbol{x}^* = -\frac{1}{\lambda_*} \boldsymbol{H}^{-1} \left(\boldsymbol{g}^T + v_* \boldsymbol{b} \right)$$

where λ_* *and* v_* *are defined by*

$$\begin{aligned} v_* &= \left(\frac{\lambda_* c - r}{s} \right)_+ \\ \lambda_* &= \arg\max_{\lambda \geq 0} \begin{cases} f_a(\lambda) \triangleq \frac{1}{2\lambda} \left(\frac{r^2}{s} - q \right) + \frac{\lambda}{2} \left(\frac{c^2}{s} - \delta \right) - \frac{rc}{s} & \text{if } \lambda c - r > 0 \\ f_b(\lambda) \triangleq -\frac{1}{2} \left(\frac{q}{\lambda} + \lambda \delta \right) & \text{otherwise} \end{cases} \end{aligned}$$

where $\boldsymbol{q} = \boldsymbol{g}^T \boldsymbol{H}^{-1} \boldsymbol{g}$, $\boldsymbol{r} = \boldsymbol{g}^T \boldsymbol{H}^{-1} \boldsymbol{b}$, *and* $\boldsymbol{s} = \boldsymbol{b}^T \boldsymbol{H}^{-1} \boldsymbol{b}$.

Furthermore, let $\Lambda_a \triangleq \{\lambda \mid \lambda c - r > 0, \lambda \geq 0\}$, *and* $\Lambda_b \triangleq \{\lambda \mid \lambda c - r \leq 0, \lambda \geq 0\}$. *The value of* λ_* *satisfies*

$$\lambda_* \in \left\{ \lambda_*^a \triangleq \text{Proj}\left(\sqrt{\frac{q - r^2/s}{\delta - c^2/s}}, \Lambda_a \right), \lambda_*^b \triangleq \text{Proj}\left(\sqrt{\frac{q}{\delta}}, \Lambda_b \right) \right\} \tag{B.1}$$

where $\lambda_* = \lambda_*^a$ *if* $f_a\left(\lambda_*^a\right) > f_b\left(\lambda_*^b\right)$ *and* $\lambda_* = \lambda_*$ *otherwise, and* $\text{Proj}(a, \boldsymbol{S})$ *is the projection of a point* x *on to a set* $\boldsymbol{S}$. *Note the projection of a point* $x \in \mathbb{R}$ *onto a convex segment of* $\mathbb{R}$, $[a, b]$, *has value* $\text{Proj}(x, [a, b]) = \max(a, \min(b, x))$.

Proof. See [2] (Appendix 10.2). □

References

[1] Naoki Abe, Prem Melville, Cezar Pendus, Chandan K Reddy, David L Jensen, Vince P Thomas, James J Bennett, Gary F Anderson, Brent R Cooley, Melissa Kowalczyk, et al. Optimizing debt collections using constrained reinforcement learning. In *Proceedings of the 16th ACM SIGKDD international conference on Knowledge discovery and data mining*, pages 75–84, 2010.

[2] Joshua Achiam, David Held, Aviv Tamar, and Pieter Abbeel. Constrained policy optimization. In *International Conference on Machine Learning*, pages 22–31. PMLR, 2017.

[3] Matthias Althoff, Andrea Giusti, Stefan B Liu, and Aaron Pereira. Effortless creation of safe robots from modules through self-programming and self-verification. *Science Robotics*, 4(31), 2019.

[4] Eitan Altman. *Constrained Markov decision processes*, volume 7. CRC Press, 1999.

[5] Aaron D Ames, Xiangru Xu, Jessy W Grizzle, and Paulo Tabuada. Control barrier function based quadratic programs for safety critical systems. *IEEE Transactions on Automatic Control*, 62(8):3861–3876, 2016.

[6] Rakesh P Borase, DK Maghade, SY Sondkar, and SN Pawar. A review of pid control, tuning methods and applications. *International Journal of Dynamics and Control*, 9(2):818–827, 2021.

[7] Urs Borrmann, Li Wang, Aaron D Ames, and Magnus Egerstedt. Control barrier certificates for safe swarm behavior. *IFAC-PapersOnLine*, 48(27):68–73, 2015.

[8] Greg Brockman, Vicki Cheung, Ludwig Pettersson, Jonas Schneider, John Schulman, Jie Tang, and Wojciech Zaremba. Openai gym, 2016.

[9] Lukas Brunke, Melissa Greeff, Adam W Hall, Zhaocong Yuan, Siqi Zhou, Jacopo Panerati, and Angela P Schoellig. Safe learning in robotics: From learning-based control to safe reinforcement learning. *Annual Review of Control, Robotics, and Autonomous Systems*, 5, 2021.

[10] Sandeep Chinchali, Pan Hu, Tianshu Chu, Manu Sharma, Manu Bansal, Rakesh Misra, Marco Pavone, and Sachin Katti. Cellular network traffic scheduling with deep reinforcement learning. In *Thirty-second AAAI conference on artificial intelligence*, 2018.

[11] Yinlam Chow, Mohammad Ghavamzadeh, Lucas Janson, and Marco Pavone. Risk-constrained reinforcement learning with percentile risk criteria. *The Journal of Machine Learning Research*, 18(1):6070–6120, 2017.

[12] Yinlam Chow, Ofir Nachum, Edgar Duenez-Guzman, and Mohammad Ghavamzadeh. A lyapunov-based approach to safe reinforcement learning. *arXiv preprint arXiv:1805.07708*, 2018.

[13] Yinlam Chow, Ofir Nachum, Aleksandra Faust, Edgar Duenez-Guzman, and Mohammad Ghavamzadeh. Lyapunov-based safe policy optimization for continuous control. *arXiv preprint arXiv:1901.10031*, 2019.

[14] Tianshu Chu, Jie Wang, Lara Codecà, and Zhaojian Li. Multi-agent deep reinforcement learning for large-scale traffic signal control. *IEEE Transactions on Intelligent Transportation Systems*, 21(3):1086–1095, 2019.

[15] Agostino De Santis, Bruno Siciliano, Alessandro De Luca, and Antonio Bicchi. An atlas of physical human–robot interaction. *Mechanism and Machine Theory*, 43(3):253–270, 2008.

[16] Christian Schroeder de Witt, Tarun Gupta, Denys Makoviichuk, Viktor Makoviychuk, Philip HS Torr, Mingfei Sun, and Shimon Whiteson. Is independent learning all you need in the starcraft multi-agent challenge? *arXiv preprint arXiv:2011.09533*, 2020.

[17] Xiaotie Deng, Yuhao Li, David Henry Mguni, Jun Wang, and Yaodong Yang. On the complexity of computing markov perfect equilibrium in general-sum stochastic games. *arXiv preprint arXiv:2109.01795*, 2021.

[18] Javier Garcıa and Fernando Fernández. A comprehensive survey on safe reinforcement learning. *Journal of Machine Learning Research*, 16(1):1437–1480, 2015.

[19] Shangding Gu, Guang Chen, Zhang Lijun, Hou Jin, Bai Yingbai, and Alois Knoll. Motion planning for automated driving with constrained reinforcement learning. *researchgate*, 2022.

[20] Shangding Gu, Jakub Grudzien Kuba, Munning Wen, Ruiqing Chen, Ziyan Wang, Zheng Tian, Jun Wang, Alois Knoll, and Yaodong Yang. Multi-agent constrained policy optimisation. *arXiv preprint arXiv:2110.02793*, 2021.

[21] Jakub Grudzien Kuba, Ruiqing Chen, Munning Wen, Ying Wen, Fanglei Sun, Jun Wang, and Yaodong Yang. Trust region policy optimisation in multi-agent reinforcement learning. *arXiv preprint arXiv:2109.11251*, 2021.

[22] Jakub Grudzien Kuba, Muning Wen, Yaodong Yang, Linghui Meng, Shangding Gu, Haifeng Zhang, David Henry Mguni, and Jun Wang. Settling the variance of multi-agent policy gradients. *arXiv preprint arXiv:2108.08612*, 2021.

[23] Qinwu Liao, Chaoli Wang, and Yingchun Mei. Sliding mode control for multi-robot formation. In *2008 IEEE Conference on Robotics, Automation and Mechatronics*, pages 395–398. IEEE, 2008.

[24] Timothy P Lillicrap, Jonathan J Hunt, Alexander Pritzel, Nicolas Heess, Tom Erez, Yuval Tassa, David Silver, and Daan Wierstra. Continuous control with deep reinforcement learning. *arXiv preprint arXiv:1509.02971*, 2015.

[25] Chenyi Liu, Nan Geng, Vaneet Aggarwal, Tian Lan, Yuan Yang, and Mingwei Xu. Cmix: Deep multi-agent reinforcement learning with peak and average constraints. In *Joint European Conference on Machine Learning and Knowledge Discovery in Databases*, pages 157–173. Springer, 2021.

[26] Songtao Lu, Kaiqing Zhang, Tianyi Chen, Tamer Basar, and Lior Horesh. Decentralized policy gradient descent ascent for safe multi-agent reinforcement learning. In *Proceedings of the AAAI Conference on Artificial Intelligence*, volume 35, pages 8767–8775, 2021.

[27] Carlos E Luis, Marijan Vukosavljev, and Angela P Schoellig. Online trajectory generation with distributed model predictive control for

multi-robot motion planning. *IEEE Robotics and Automation Letters*, 5(2):604–611, 2020.

[28] Xiaobai Ma, Jiachen Li, Mykel J Kochenderfer, David Isele, and Kikuo Fujimura. Reinforcement learning for autonomous driving with latent state inference and spatial-temporal relationships. In *2021 IEEE International Conference on Robotics and Automation (ICRA)*, pages 6064–6071. IEEE, 2021.

[29] Viktor Makoviychuk, Lukasz Wawrzyniak, Yunrong Guo, Michelle Lu, Kier Storey, Miles Macklin, David Hoeller, Nikita Rudin, Arthur Allshire, Ankur Handa, et al. Isaac gym: High performance gpu-based physics simulation for robot learning. *arXiv preprint arXiv:2108.10470*, 2021.

[30] Teodor Mihai Moldovan and Pieter Abbeel. Safe exploration in markov decision processes. In *Proceedings of the 29th International Coference on International Conference on Machine Learning*, pages 1451–1458, 2012.

[31] NVIDIA. Nvidia physx. *https://developer.nvidia.com/physx-sdk*, 2020.

[32] Bei Peng, Tabish Rashid, Christian A Schroeder de Witt, Pierre-Alexandre Kamienny, Philip HS Torr, Wendelin Böhmer, and Shimon Whiteson. Facmac: Factored multi-agent centralised policy gradients. *arXiv preprint arXiv:2003.06709*, 2020.

[33] David Pollard. Asymptopia: an exposition of statistical asymptotic theory. 2000. *URL http://www. stat. yale. edu/pollard/Books/Asymptopia*, 2000.

[34] Zengyi Qin, Kaiqing Zhang, Yuxiao Chen, Jingkai Chen, and Chuchu Fan. Learning safe multi-agent control with decentralized neural barrier certificates. In *International Conference on Learning Representations*, 2020.

[35] Tabish Rashid, Mikayel Samvelyan, Christian Schroeder, Gregory Farquhar, Jakob Foerster, and Shimon Whiteson. Qmix: Monotonic value function factorisation for deep multi-agent reinforcement learning. In *International Conference on Machine Learning*, pages 4295–4304. PMLR, 2018.

[36] Alex Ray, Joshua Achiam, and Dario Amodei. Benchmarking safe exploration in deep reinforcement learning. *arXiv preprint arXiv:1910.01708*, 7, 2019.

[37] Mikayel Samvelyan, Tabish Rashid, Christian Schroeder De Witt, Gregory Farquhar, Nantas Nardelli, Tim GJ Rudner, Chia-Man Hung, Philip HS Torr, Jakob Foerster, and Shimon Whiteson. The starcraft multi-agent challenge. *arXiv preprint arXiv:1902.04043*, 2019.

[38] John Schulman, Sergey Levine, Pieter Abbeel, Michael Jordan, and Philipp Moritz. Trust region policy optimization. In *International conference on machine learning*, pages 1889–1897. PMLR, 2015.

[39] John Schulman, Filip Wolski, Prafulla Dhariwal, Alec Radford, and Oleg Klimov. Proximal policy optimization algorithms. *arXiv preprint arXiv:1707.06347*, 2017.

[40] Shai Shalev-Shwartz, Shaked Shammah, and Amnon Shashua. Safe, multi-agent, reinforcement learning for autonomous driving. *arXiv preprint arXiv:1610.03295*, 2016.

[41] David Silver, Aja Huang, Chris J Maddison, Arthur Guez, Laurent Sifre, George Van Den Driessche, Julian Schrittwieser, Ioannis Antonoglou, Veda Panneershelvam, Marc Lanctot, et al. Mastering the game of go with deep neural networks and tree search. *nature*, 529(7587):484–489, 2016.

[42] Richard S Sutton and Andrew G Barto. *Reinforcement learning: An introduction*. MIT press, 2018.

[43] Chao Yu, Akash Velu, Eugene Vinitsky, Yu Wang, Alexandre Bayen, and Yi Wu. The surprising effectiveness of mappo in cooperative, multi-agent games. *arXiv preprint arXiv:2103.01955*, 2021.

[44] Moritz A. Zanger, Karam Daaboul, and J. Marius Zöllner. Safe continuous control with constrained model-based policy optimization, 2021.

[45] Wenbo Zhang, Osbert Bastani, and Vijay Kumar. Mamps: Safe multi-agent reinforcement learning via model predictive shielding. *arXiv preprint arXiv:1910.12639*, 2019.

[46] Xiangyu Zhao, Changsheng Gu, Haoshenglun Zhang, Xiwang Yang, Xiaobing Liu, Hui Liu, and Jiliang Tang. Dear: Deep reinforcement learning for online advertising impression in recommender systems. In *Proceedings of the AAAI Conference on Artificial Intelligence*, volume 35, pages 750–758, 2021.

[47] Yuke Zhu, Josiah Wong, Ajay Mandlekar, and Roberto Martín-Martín. robosuite: A modular simulation framework and benchmark for robot learning. *arXiv preprint arXiv:2009.12293*, 2020.